Am J Physiol Cell Physiol 313: C516–C532, 2017.
First published August 16, 2017; doi:10.1152/ajpcell.00106.2017.

REVIEW

Molecular insights into the normal operation, regulation, and multisystemic roles of K^+-Cl^- cotransporter 3 (KCC3)

A. P. Garneau,[1,2] A. A. Marcoux,[1] R. Frenette-Cotton,[1] F. Mac-Way,[1] J. L. Lavoie,[2] and P. Isenring[1]

[1]*Nephrology Research Group, Department of Medicine, Laval University, Quebec City, Quebec, Canada; and*
[2]*Cardiometabolic Axis, Kinesiology Department, University of Montréal, Montreal, Quebec, Canada*

Submitted 11 May 2017; accepted in final form 14 August 2017

Garneau AP, Marcoux AA, Frenette-Cotton R, Mac-Way F, Lavoie JL, Isenring P. Molecular insights into the normal operation, regulation, and multisystemic roles of K^+-Cl^- cotransporter 3 (KCC3). *Am J Physiol Cell Physiol* 313: C516–C532, 2017. First published August 16, 2017; doi:10.1152/ajpcell.00106.2017.—Long before the molecular identity of the Na^+-dependent K^+-Cl^- cotransporters was uncovered in the mid-nineties, a Na^+-independent K^+-Cl^- cotransport system was also known to exist. It was initially observed in sheep and goat red blood cells where it was shown to be ouabain-insensitive and to increase in the presence of *N*-ethylmaleimide (NEM). After it was established between the early and mid-nineties, the expressed sequence tag (EST) databank was found to include a sequence that was highly homologous to those of the Na^+-dependent K^+-Cl^- cotransporters. This sequence was eventually found to code for the Na^+-independent K^+-Cl^- cotransport function that was described in red blood cells several years before. It was termed KCC1 and led to the discovery of three isoforms called KCC2, KCC3, and KCC4. Since then, it has become obvious that each one of these isoforms exhibits unique patterns of distribution and fulfills distinct physiological roles. Among them, KCC3 has been the subject of great attention in view of its important role in the nervous system and its association with a rare hereditary sensorimotor neuropathy (called Andermann syndrome) that affects many individuals in Quebec province (Canada). It was also found to play important roles in the cardiovascular system, the organ of Corti, and circulating blood cells. As will be seen in this review, however, there are still a number of uncertainties regarding the transport properties, structural organization, and regulation of KCC3. The same is true regarding the mechanisms by which KCC3 accomplishes its numerous functions in animal cells.

CCC; cation-Cl^- cotransporter; KCC; K^+-Cl^- cotransporter; Andermann syndrome; animal models

K^+-CL^- COTRANSPORTER 3 (KCC3) is a membrane protein that belongs to the cation-Cl^- cotransporter (CCC) family along with three other closely related isoforms called KCC1, KCC2, and KCC4 (Fig. 1). It is also called SLC12A6 according to the HUGO nomenclature. Its main function is to facilitate the translocation of K^+ and Cl^- across the surface of many cell types, and unlike certain of the other CCC family members, its activity is entirely Na^+-independent (57, 96). Even if the existence of a K^+-Cl^- cotransport system has been uncovered in the late seventies (14, 38, 71) and its characteristics examined at length since then, the subgroup of proteins responsible for this process was only uncovered in the late nineties, approximately five years after the first CCC family members were identified.

In the last two decades, it has become increasingly apparent that KCC3 plays important physiological roles in many tissues. It has also become apparent that even if this member of the KCC subfamily is widely distributed in any given animal species and is present in certain cell types along with KCC1, KCC2 or KCC4, its overall pattern of distribution is still relatively unique. Although it is perhaps still unclear based on the current literature, the same will probably hold true regarding the operational characteristics of KCC3, its functional purpose within specific systems, and the molecular mechanisms or environmental factors through which its activity is affected.

This review will focus on the molecular features and physiological roles of KCC3 in animal species. Those of various CCCs will also be tackled on occasion, but only to draw relevant inferences on KCC3 itself or to highlight potentially important differences between this isoform and the other isoforms. Otherwise, the proposed recapitulation is not intended

Address for reprint requests and other correspondence: P. Isenring, L'Hôtel-Dieu de Québec Institution, 10, rue McMahon, Québec (Qc), Canada G1R 2J6 (e-mail: paul.isenring@crhdq.ulaval.ca).

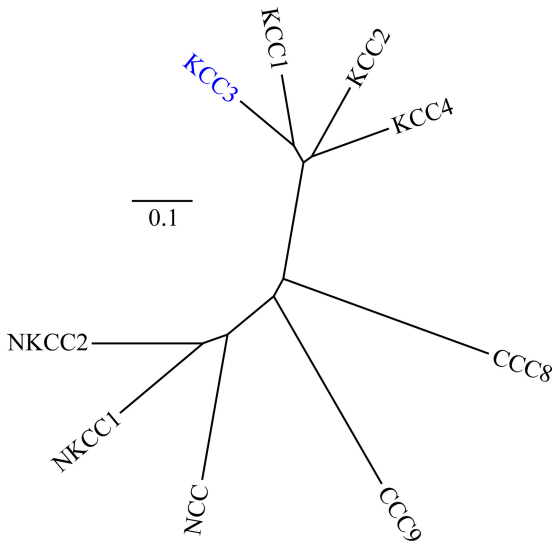

Fig. 1. Phylogenetic tree of the cation-Cl^- cotransporter (CCC) family. The cladogram was generated with the programs Clustal Omega and FigTree v1.4.3 (97) using the longest human amino acid sequences for all of the CCCs included in the analysis. Potassium-chloride cotransporter type 3 (KCC3) has evolved from a common ancestor in bacterium and falls into one of four clades, that is, in the Na^+-independent K^+-coupled Cl^- cotransporters. Scale is in genetic distance. NKCC1, NP_001037.1; NKCC2, NP_000329.2; NCC, NP_000330.2; KCC1, NP_005063.1; KCC2, NP_001128243.1; KCC3, NP_598408.1; KCC4, NP_006589.2; CCC8, NP_064631.2; CCC9, NP_078904.3.

to cover all of the approaches through which KCC3 has been characterized or all of the functions it has been ascribed. From reading the following document, it will appear nonetheless evident that much work still needs to be accomplished before a more integrated picture on the molecular mechanisms of KCC3-mediated K^+-Cl^- cotransport is conceived.

KCC3, A COTRANSPORTER WITH MANY FACES

Place of KCC3 in the CCC Family, Historical Considerations, and Splice Variants

As shown in Fig. 1, KCC3 falls into a distinct phylogenetic clade within the CCC family and it does so along with KCC1 (SLC12A4), KCC2 (SLC12A5), and KCC4 (SLC12A7). As for the other CCCs, they fall into three supplementary clades. One includes the Na^+-dependent Cl^- transporters, that is, secretory or housekeeping NKCC1 (SLC12A2), absorptive or renal Na^+-K^+-Cl^- cotransporter (NKCC2; SLC12A1), and renal Na^+-Cl^- cotransporter (NCC; SLC12A3). The other two clades include one member each, that is, CCC8 (SLC12A9) and CCC9 (SLC12A8).

The molecular identity of KCC3 was first reported by three independent research groups from December 1998 to February 1999 (time of submission). One group, Hiki et al. (57), identified KCC3 in VEGF-stimulated human umbilical vein endothelial cells (HUVECs) through differential display PCR and cloned it subsequently from a phage HUVEC library through homology-based screening. The two other groups, Race et al. (96) and Mount et al. (88), identified KCC3 in the expressed sequence tags (EST) database using KCC1 and KCC2 as queries. They cloned it afterwards through conventional PCR from a human placenta cDNA library (Race et al.) and from both a human muscle and a human brain cDNA library (Mount et al.). Note that the cDNA isolated from the muscle and brain libraries was termed KCC4 initially, but that it is now referred to as KCC3.

After its discovery, KCC3 was found to be highly homologous to the other KCCs, sharing ~73% identity in amino acid sequence with either of them, and moderately homologous to the Na^+-coupled NKCC1, sharing ~29% identity with this other transporter (Table 1). When the NH_2 terminus is excluded from the alignment studies, the identities increases to ~76 and 32%, respectively. KCC3 was also found to exist as several variants. As shown in Fig. 2, these variants are formed as follows: *1*) through alternative splicing of exon 1A (KCC3A) or 1B (KCC3B); *2*) through alternative exclusion of a first initiation site in exon A ($KCC3A_{is2}$) or a first and second initiation site in the same exon ($KCC3A_{is3}$); and *3*) through the possible exclusion of exon 2 in either of KCC3A ($KCC3A_{\Delta e2}$) and KCC3B ($KCC3B_{\Delta e2}$). Of note, KCC3A is the longest and most abundantly expressed of these splice variants.

Structure

X-ray-based structural determinations have been obtained for only one CCC family member until now (124). At the same time, the member in question was from an archea species (*Methanosarcina acetivorans)* and the protein region analyzed, the COOH terminus, only ~10%-identical compared with that of mammalian KCC3. Elseways, much of the insight gained into the tertiary organization of the CCCs was derived from in vitro analyses of animal NKCC1. More specifically, it came from the identification of phosphorylation, *N*-glycosylation and self-interacting sites within the carrier as well as from the topological localization of inserted tags within its large central domain (15, 23, 42, 52, 87, 111). Additional insight has now been obtained for the KCCs as well (36, 98, 110, 126).

Based on the Kyte-Doolittle algorithm, the hydropathy plot model of KCC3 is predicted to consist of a central core of 12 transmembrane segments (TMs) flanked by intracellular termini (see Fig. 3). Not surprisingly, it is very similar to that of the other KCCs and of the NKCCs. All of the CCC family members are indeed highly conserved, especially in their central core and COOH terminus. The only notable difference between the KCCs and the NKCCs is the position of the longest extracellular loop in which all of the putative *N*-linked glycosylation sites are localized. In KCC3; this loop is between TM5 and TM6 and in NKCC1, it is between TM7 and TM8 (see Fig. 3).

Multiple lines of evidence suggest that the Na^+- and K^+-coupled CCCs are organized in the cell membrane as homo-

Table 1. *Percentage identities in amino acid sequence between human KCC3 and human KCC1, KCC2, KCC4 or NKCC1*

Carrier	Entire Sequence, %	Central Core + COOH Terminus, %
KCC1	76.6	80.7
KCC2	71.5	74.6
KCC4	69.8	73.7
NKCC1	29.4	32.3

Alignments and identity scores were generated by the program Clustal Omega (108). KCC3, NP_598408.1; KCC1, NP_005063.1; KCC2, NP_001128243.1; KCC4, NP_006589.2; NKCC1, NP_001037.1.

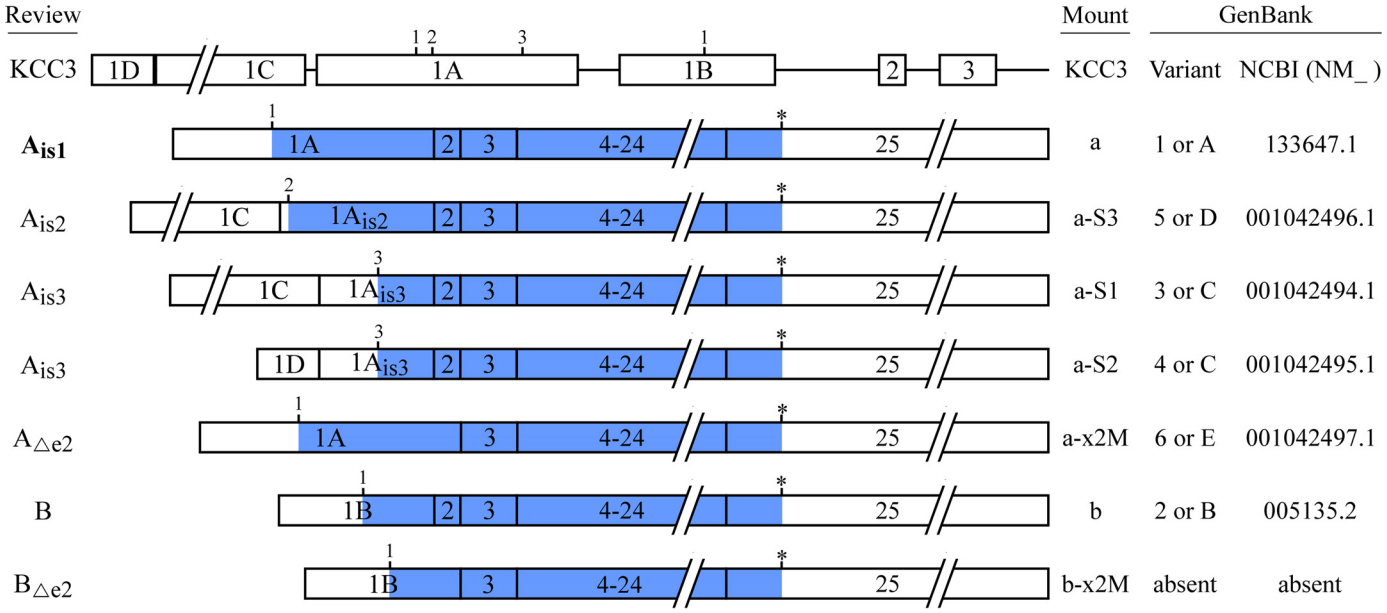

Fig. 2. KCC3 splice variants. The primary transcript counts 108,069 nucleotides. Boxes correspond to exons and lines correspond to untranslated regions. They are all drawn to scale horizontally, but those of the introns are reduced by a factor of 250. Open reading frames are indicated by blue filling. While the variants are named according to a descriptive nomenclature for this review (*left*), their original designations (88) and those used in GenBank are also provided (*right*). Numbers above the boxes correspond to initiation sites. Abbreviations: is, initiation site; *, stop codon.

oligomers, perhaps mainly as dimers, and that the COOH terminus plays a key role in carrier assembly. Part of this evidence was provided through yeast two-hybrid analyses by Simard and colleagues (110, 111) and by Brunet et al. (15), who demonstrated that the COOH termini of NKCC1, NKCC2, KCC2, and KCC4 were each endowed with self-interacting properties. Evidence was also provided through structural studies by Bergeron et al. (7), who found that KCC4 was present at the cell surface in both monomeric and homodimeric forms. Through the work of Bergeron et al., notably, it was the first time that the shape, dimensions and oligomeric state of an animal CCC were determined through a direct method, that is, through transmission electron microscopy and single particle analysis.

Convincing data to the effect that KCC3 is also organized at the cell surface as a homo-oligomer came initially from Simard et al. (110), who were able to coimmunoprecipitate c-Myc-tagged KCC3 and human *Influenza* hemagglutinin (HA)-tagged KCC3 after coexpression of the two proteins in *Xenopus laevis* oocytes. They found, in addition, that KCC3 could be immunoprecipitated with either of KCC1, KCC2, KCC4 or NKCC1, and on this basis, concluded that it could then exhibit different functional characteristics through hetero-oligomeric associations with other CCCs. In the yeast two-hybrid studies, however, Simard et al. were unable to identify self-interacting domains for KCC3. Presumably, the specific baits or preys derived from this isoform adopted a disrupted conformational state in *Saccharomyces cerevisiae* so that no associations were revealed.

Sites and Domains of Interest

Figure 3 is used to show the localization of various protein domains or consensus sites in the amino acid sequence of KCC3A, the most abundantly expressed splice variant. As

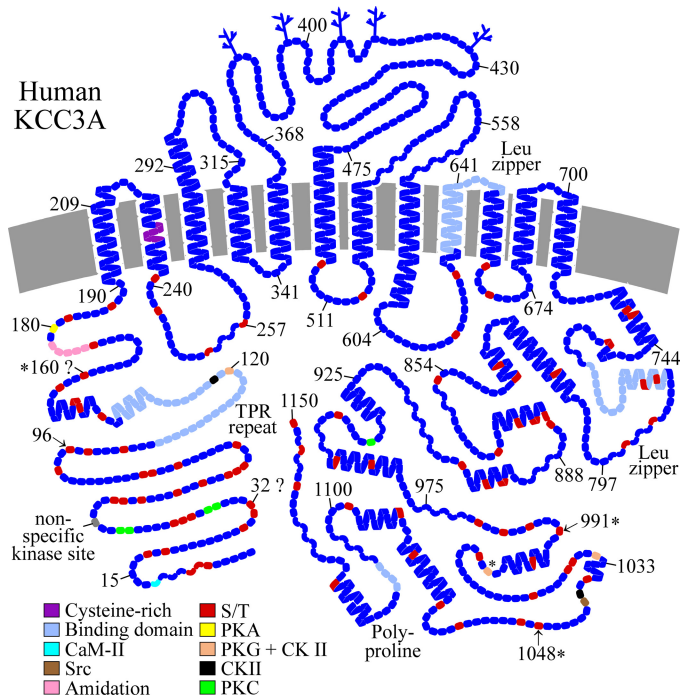

Fig. 3. Hydropathy plot model of human KCC3A. Amino acid residues are represented by round or square forms (one form per residue) and putative glycosylation sites are represented by branched lines. Other residues, canonical sites, and domains are indicated through different colors as per the legend accompanying the model. Abbreviations: *, conserved among isoforms and orthologs; ?, role inferred through indirect evidence, →, role inferred through direct evidence. Not shown: residues or canonical sites that are not expected to play a role based on their topological localization. The model was drawn by the program PLOT and canonical sites were identified through a variety of computational tools. Abbreviations: CaM, calmodulin; CK, casein kinase; PK, protein kinase; TPR, tetratricopeptide repeat domain.

described in the associated legend, it was generated through a combination of computational tools. In this figure, the sites are accompanied by the star sign if they are conserved among isoforms and orthologs, pointed by an arrow if they were shown to play a role, and adjoined with the question mark if a role was inferred through indirect indications. Excluded from the sequence displayed are canonical phosphorylation sites in the putative transmembrane domains and extracellular loops as well as canonical *N*-glycosylation sites outside of the putative extracellular loops.

As seen, multiple S/T residues and canonical phosphorylation sites are present in the cytosolic domains. Two research groups have reported that S_{96}, T_{991}, and T_{1048} correspond to actual phosphoacceptors. S_{96} was identified by Melo et al. (81) through liquid chromatography tandem-mass spectrometry (LC-MS/MS) in an epitope-tagged NH_2-terminal fragment of human KCC3A purified from *Escherichia coli*. Yet, S_{96} did not appear to play a role in carrier regulation, at least not on its own. As for T_{991} and T_{1048}, they were identified by Rinehart et al. (98) also through LC-MS/MS, but in an epitope-tagged full-length KCC3A purified from human embryonic kidney (HEK)-293 cells. Importantly, these sites were shown to be dephosphorylated under hypotonic condition and their replacement by alanine residues to increase carrier activity. In the study by Rinehart et al., additional phosphopeptides were identified under basal conditions, but their phosphorylation state was unaffected by changes in cell volume.

As also seen in Fig. 3, five putative *N*-linked glycosylation sites (N1 to N5) are present in KCC3A. However, only three of them (N1, N2, and N5) are fully conserved among isoforms and orthologs. Although KCC3 is known to be a glycoprotein (57, 88) as are the other KCCs (53, 92, 126), the sites potentially involved in glycosylation have still not been subjected to experimental confirmation. At the same time, it should be noted that Weng et al. (126) did obtain such confirmation for the four NXS/T sites (N1, N2, N3, and N5) of KCC4 through mutagenic studies. It is therefore likely that the glycosylation sites of KCC3 consist of at least N1, N2, and N5, and perhaps of the nonconserved N3 and N4 sites as well.

The other canonical sites or protein domains of potential importance in KCC3 include a tetratricopeptide repeat (TPR) and an amidation motif in the distal NH_2 terminus, a cysteine-rich stretch in TM2, an amino-acid permease box encompassing the central core, a leucine zipper in TM9 and in the proximal COOH terminus, and a polyproline-rich sequence in the distal COOH terminus. A number of them could play a role in protein-protein interactions, all the more that they are conserved among isoforms and orthologs. As for the permease domain, it is unclear at this time whether it could actually serve as a pathway for amine-containing substrates in KCC3. Yet, this possibility cannot be excluded given that Daigle et al. (22) have shown CCC9, another CCC family member, to be endowed with the ability of transporting spermidine and spermine across the cell membrane.

Expression and Distribution

Expression patterns inferred from the human EST databank show that KCC3 is widely distributed, that is, present in 34 different tissues out of the 45 for which a library was generated. They also show relatively high transcript abundance in many of these tissues. For instance, there are more than 37 messages per million (MPM) in (by decreasing order of abundance) testis, bone, cervix, adipose tissue, mouth, pituitary, esophagus, pharynx, salivary gland, parathyroid, thyroid, bone marrow, vascular tissues, spleen, and thymus. KCC3 is also expressed in brain and kidney (24 and 28 MPM, respectively) as well as in heart and skeletal muscle (11 and 9 MPM, respectively). Based again on the human EST databank, KCC3 is not detected in adrenal gland, ear, or peripheral nerve. Further localization studies, however, did show that this isoform was present in such structures but confined to a limited number of specialized cell types within them (13, 50, 93, 100).

Multiple tissue Northern and Western blot analyses have also revealed wide distribution of KCC3 in human (57, 88, 96), but expression levels were higher in brain, heart, kidney, and skeletal muscle. While KCC3 was found to be widely distributed in mouse as well (13, 93), its relative abundance in lung was higher compared with human. Otherwise, studies in single cell types or cells lines have shown that KCC3 was expressed in mouse and human erythrocytes (90), rat vascular smooth muscle cells (VSMCs; 34), human colonocytes, leucocytes, and melanocytes (96), VEGF-stimulated HUVECs (57) as well as in mouse sciatic axons (13, 16) and hippocampal neurons (13, 16, 93).

As for the compartmental localization of KCC3 inside various tissues, organs, and cells, it has been mainly examined in the central (CNS) and peripheral nervous system (PNS), kidney, arterial tree, inner ear, adrenal gland, and blood. In particular, the protein has been detected in the hippocampus, cerebral cortex, cerebellum, spinal dorsal root ganglion, sciatic nerve, aortic VSMCs, mesenteric and saphenous arterial VSMCs, organ of Corti, medullary adrenal gland, and basolateral membrane of proximal renal tubular cells (13, 50, 80, 93, 104). As for the subcellular sites of expression, they have been shown to include various organelles as well as the plasmalemma (45, 101, 115).

Characteristics of Ion Transport

By and large, the main transport role of KCC3 is probably similar to that of the other subfamily members, that is, to promote the electroneutral transmembrane symport of K^+ and Cl^- ions in a 1:1 stoichiometric ratio. For instance, Jennings et al. (63) have shown that in rabbit erythrocytes, where KCC3 is more abundant than the other Na^+-independent CCCs (90, 99), the ratio of KCC-specific K^+ efflux to KCC-specific Cl^- efflux at a clamped membrane potential of 0 mV was 1.12 ± 0.26. In various studies, furthermore, the dependence of KCC-dependent K^+ transport or Cl^- transport on extracellular K^+ concentration ($[K^+]_e$) and $[Cl^-]_e$ was generally described by a single-site binding model for each of the transported ions (83, 84, 91, 113). This has been shown to be the case for KCC3 as well (83, 84).

Based on the studies available, however, it is unclear whether the number of ions translocated per transport cycle is $1K^+$:$1Cl^-$, $2K^+$:$2Cl^-$, $3K^+$:$3Cl^-$ or more. In some of these studies, for instance, transport activities at the 0 mM concentration point were not always determined experimentally (84). In addition, the activities versus $[ion]_e$ relationships were not fitted with a Hill-type four-parameter equation, but with the Michaelis-Menten equation. Yet, they would have been more

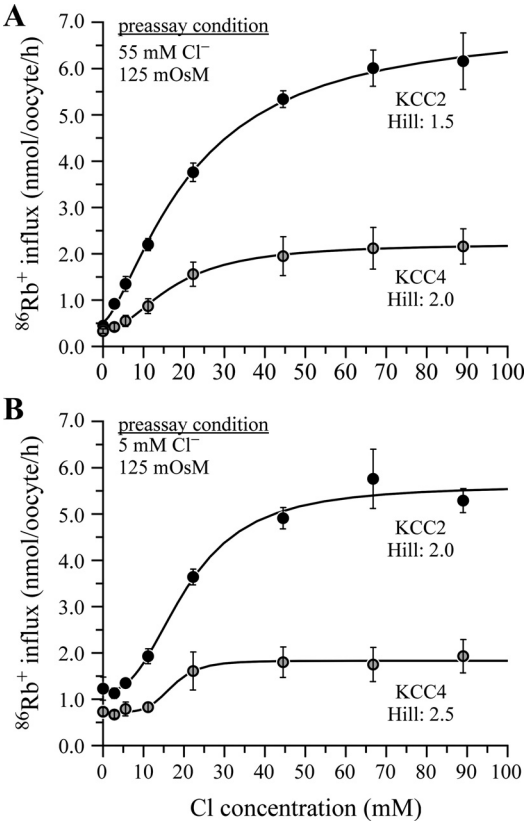

Fig. 4. Effect of changes in $[Cl^-]_i$ on KCC4 activity as a function of external $[Cl^-]$. Oocytes were first incubated in 5 mM or 55 mM Cl^- for 1 h. They were subsequently assayed for $^{86}Rb^+$ transport activity at different $[Cl^-]_e$ over 45 min. Data are presented as mean background-subtracted measurements among 4 experiments using 8 oocytes per condition in each experiment. Curves were fitted through least square analysis using a 4-parameter Hill-type equation. Between 5 mM and 55 mM Cl^-, Hill coefficients were statistically different. The data shown in this figure are from unpublished experiments.

adequately fitted through Hill coefficients of more than one (see Figure 6D in Reference 83 for KCC1 and Figure 3D in Reference 10 for KCC4). Frenette-Cotton et al. (44) have also observed through additional experiments that the number of apparent Cl^- transport sites in certain KCCs was higher than one, and that for an unknown reason, it increased even further when carrier activity was measured after intracellular Cl^- concentration ($[Cl^-]_i$) reduction (see Fig. 4 in this review).

Even if such studies had consistently revealed Hill coefficients of 1.0 as determined through least squares analysis, it should be remembered that the presence of multiple binding sites for the same ion in a multiporter system will only be revealed through kinetic determinations if such sites share similar affinities for this ion (61, 62). As it stands, moreover, experimental evidence to confirm that K^+-Cl^- cotransport is electroneutral under all circumstances or for all of the KCCs is unavailable. The possibility of alternate transport stoichiometries would appear even more likely if, as was previously described for NKCC1 (77), substrate translocation by the KCCs could also proceed despite incomplete reactions.

The kinetic characteristics of KCC3 and of the other isoforms have been examined primarily in the *X. laevis* oocyte expression system. Nonetheless, the data reported thus far are probably physiologically relevant given that these cells have generally been shown to reproduce the in vivo characteristics of other foreign transport proteins rather accurately (109). It was found that in comparison to KCC1 and KCC4, KCC3 exhibited the same affinity for K^+ (~20 mM), NH_4^+ (~20 mM), or Cl^- (~50 mM), but much higher transport capacity (10, 53, 83, 84). It was also found that KCC3 was inhibited by cell shrinking, low $[Cl^-]_i$, paraphysiological pH_i levels ($>$7.25 and $<$6.75), furosemide (K_i in the low μM range), and [(dihydroindenyl)oxy]alkanoic acid (DIOA); relatively resistant to inhibition by bumetanide (K_i in the high μM range); and activated by cell swelling, high $[Cl^-]_i$, and *N*-ethylmaleimide (NEM) (83, 84, 96, 107).

If the transport stoichiometry of KCC3 is in fact $1K^+$:$1Cl^-$, net ion transport by this carrier is expected to be outwardly directed. Indeed, $[K^+]_i$-to-$[K^+]_e$ ratios commonly found in tissues are over 25 (see Table 2) so that when $[Cl^-]_e$ is 100 mM, a $[Cl^-]_i$ of 4 mM or more will be associated with net ion efflux. Yet, $[K^+]_e$ can reach much higher levels in certain tissues or during certain processes such as cell repolarization, so that an even higher $[Cl^-]_i$ could also be associated with net ion influx. As for NH_4^+-Cl^- movement by KCC3, it is expected to be inwardly directed given that $[NH_4^+]_i$-to-$[NH_4^+]_e$ ratios are below two in most tissues (40, 54, 95, 121). Despite such predictions, however, it should be noted that ion movement by the K^+-Cl^- cotransport system is not perfectly symmetrical, at least not in the low-K^+ sheep erythrocyte model where it is in fact outwardly poised even at equilibrium (30). The efficiency of KCC3 as an influx system could thus be lower than expected.

Activation of KCC3 is expected to generate several effects inside and outside the cellular environment. Examples of changes induced in this setting (some of which are illustrated in Fig. 5) are as follows: *1*) osmotically driven outward movement of water through the aquaporins causing the cell to dehydrate (25); *2*) decreases in $[K^+]_i$, $[Cl^-]_i$, and $[H^+]_i$ affecting the activity of K^+-, Cl^--, and pH-sensitive proteins such as ion transport systems and growth factors (10, 13, 128); *3*) increases in $[K^+]_e$, $[Cl^-]_e$, and $[H^+]_e$ causing many additional effects. Given that KCC3 in polarized cells has been found to be basolaterally disposed thus far (45, 49, 80, 84), activation of K^+-Cl^- efflux in various epithelia

Table 2. *$[Cl^-]_i$, $[K^+]_i$, $[Cl^-]_e$, and $[K^+]_e$ in selected human cell types*

	$[Na^+]_e$	$[Na^+]_i$	$[Na^+]_{e/i}$	$[K^+]_e$	$[K^+]_i$	$[K^+]_{i/e}$	$[Cl^-]_e$	$[Cl^-]_i$	$[Cl^-]_{e/i}$	Ref.
Cardiomyocyte (relaxed)	140.0	10.0	14	4.0	140.0	35.0	120.0	30.0	4.0	(74)
Smooth muscle cell	137.0	9.0	15.2	5.0	165.0	33.0	134.0	55.0	2.4	(74)
Red blood cell	145.0	11.0	13.2	4.5	140.0	31.1	116.0	80.0	1.5	(58)
Neuron	142.0	14.0	10.1	4.5	120.0	26.7	107.0	8.0	13.4	(56)

The data shown were obtained from multiples sources as indicated in the Table.

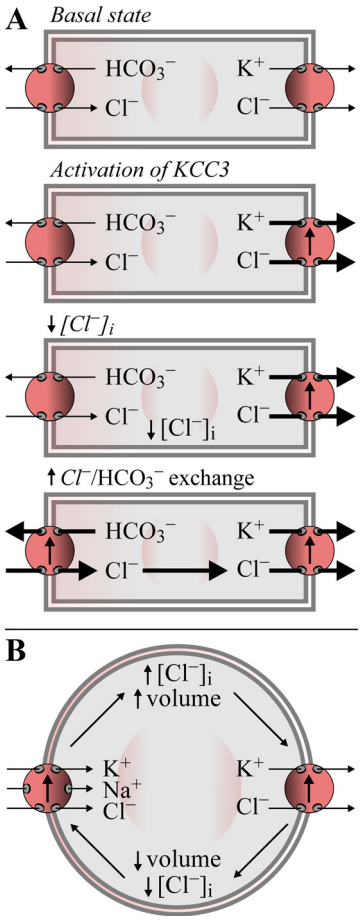

Fig. 5. Examples of interaction between KCC3 and other transport systems. *A*: Cl^-/HCO_3^- exchanger. Activation of KCC3 causes $[Cl^-]_i$ to decrease so that the driving force for inward Cl^- movement is increased and the HCO_3^- is driven out of the cell in exchange for Cl^-. *B*: NKCC1 activation of KCC3 causes $[Cl^-]_i$ to decrease so that water is osmotically driven out of the cell. Through the decrease in $[Cl^-]_i$ and cell volume, NKCC1 is activated secondarily and causes $[Cl^-]_i$ to increase so that water is osmotically driven into the cell. Through the increase in $[Cl^-]_i$ and cell volume, KCC3 is activated secondarily.

should also be associated with net Cl^-, Na^+, and water reabsorption in most tissues (25, 47, 69, 86).

The Na^+-dependent cotransporter NKCC1 is often expressed in the same cell types as KCC3 (54, 89, 120). Although these carriers both belong to the CCC family and share common transport roles overall, they nonetheless display reciprocal functional properties (49, 89). For instance, NKCC1 generally promotes net inward Cl^- movement rather than outward Cl^- movement, is more active at low $[Cl^-]_i$ rather than at high $[Cl^-]_i$, and is induced by cell shrinking rather than cell swelling. As illustrated in Fig. 5, expression of NKCC1 and KCC3 in the same cell type would therefore imply that activation of one transporter could lead to upregulation of the other and, accordingly, that inhibition of one transporter could lead to downregulation of the other. It would also imply that these transporters could counteradjust the effect of each other to prevent excessive volume regulatory responses or changes in cellular ion concentration induced by either of them.

Regulation of KCC3 and of Other Subfamily Members

The mechanisms of KCC3 regulation have been introduced in section *Sites and Domains of Interest*. As it stands, they are generally presumed to be analogous with those of the other Na^+-independent CCCs, that is, to involve the same group of regulatory targets as well as intermediates and to alter carrier activity through similar effects. Yet, this rule does not apply entirely to KCC2, also referred to as neuron-specific KCC, in that K^+-Cl^- cotransport by this subfamily member is not highly sensitive to changes in cell volume even when it is analyzed in a nonneuronal cell expression system (91, 113, 114). Such a rule probably does not entirely apply to KCC3 either, but future studies will be required to prove it incorrect.

The environmental factors through which KCC3 activity is affected have also been introduced in previous sections. It is generally postulated that they affect cotransporter function through posttranslational modifications. More specifically, inactivation of K^+-Cl^- cotransport is believed to occur through carrier phosphorylation by protein kinases (PKs) and activation to occur through carrier dephosphorylation by protein phosphatases (PPs). This model has been initially deduced from the effect of pharmacological agents on KCC activity during changes in cell volume (3, 27, 72, 105). It is now supported by the identification of phosphoacceptor sites in the COOH terminus of KCC3 (T_{991} and T_{1048}) and the observation that native KCC3 in human red blood cells is dephosphorylated at these sites during cell swelling (98).

The kinases potentially involved in KCC3 downregulation include members of the with-no-lysine (WNK) protein kinase family, of which four different isoforms are known to exist, as well as SPS1-related proline/alanine-rich kinase (SPAK) or oxidative stress response kinase (OSR1). In many studies, all of the WNK kinases have been found to inhibit KCC3 (28, 51, 64, 81, 82, 98), and based on two such studies, to exert this effect by phosphorylating the carrier via SPAK at residue S_{96} (81) as well as at residue T_{1048} (28). Yet, there is evidence to suggest that SPAK can affect cation-Cl^- cotransport even when it is unable to interact with a CCC (94). In addition, Frenette-Cotton et al. (44) have found that inhibition of KCC4 activity by WNK4 was SPAK-insensitive in *X. laevis* oocytes and that its phosphorylation state was unaffected by either of these enzymes. Whether the same will hold true for KCC3 in this expression system remains to be confirmed.

Other kinases have been found to play a role in regulation of K^+-Cl^- cotransport, but most of the studies carried out thus far have not been concerned with KCC3 per se. PKC is nonetheless a potential candidate given that phorbol esters have been found to exert an inhibitory effect on K^+-Cl^- cotransport by native KCCs and by mouse KCC4 expressed in *X. laevis* oocytes (8, 9, 55). However, mutagenic studies have revealed that this effect was not mediated through phosphorylation of putative PKC sites within the carrier, at least not for KCC4. Elseways, there also are reasonable indications for the involvement of PKG in KCC1 and KCC4 regulation as well as tyrosine kinases in KCC2 regulation (2, 32, 34, 125). Their involvement in KCC3 regulation is therefore a possibility to entertain as well.

As for the phosphatase at play, its molecular identity is still uncertain. Given that cell swelling-induced KCC3 activation is sensitive to calyculin A but insensitive to okadaic acid, it is

likely to consist of a PP1 family member (29, 51, 84, 105). More recently, a study by Frenette-Cotton et al. (44) in *X. laevis* oocytes showed that for KCC4, PP1α and PP1γ1 were probably the enzymes involved, but that abrogation of WNK kinase activity was necessary for K^+-Cl^- cotransport to be induced by PP1 activity under isotonic conditions. While it was already known that these enzymes affected K^+-Cl^- cotransport through a common pathway, Frenette-Cotton et al. have found that the kinase acted on the phosphatase to inhibit K^+-Cl^- cotransport during cell swelling and not the other way around as suggested previously (48, 75).

In the study of Frenette-Cotton et al. (44), intriguingly, cell swelling-induced KCC4 activation was seen to be associated with a clear increase in carrier phosphorylation rather than carrier dephosphorylation. At the same time, their approach was not to examine the phosphorylation state of individual residues as in other studies (28, 81, 98), but that of the entire protein. These observations point to the existence of additional phosphoacceptor sites in the KCCs, KCC3 included, and imply that their phosphorylation by a yet unidentified kinase could cause K^+-Cl^- cotransport to be induced. Not inconceivably, the accessibility of such sites could depend on the phosphorylation state of other sites such as T_{991} and T_{1048} in the COOH terminus of KCC3.

Aside from the phosphoregulatory enzymes mentioned in this section, there are several lines of evidence to suggest that the cytoskeletal network is involved in regulation of KCC3 as well (2, 46, 102). For instance, Salin-Cantegrel et al. (102) have shown that in order to be activated in cervical cancer cells, the carrier needed to associate with Vav2, a guanine nucleotide exchange factor (GEF) involved in Rho GTPase-dependent actin remodeling. More specifically, they found that when these cells were swollen in tissue culture plates, they formed actin-rich protruding lamellipodia in which KCC3 colocalized with the active form of *Vav2* at their surface. They also found that the carrier-GEF interaction was supported by the COOH terminus of both proteins, namely, by a polyproline-rich domain in KCC3 and a Src-homology 3 (SH3) domain in *Vav2*.

Kcc3 Is Responsible for Andermann Syndrome

In the early 2000s, a collaborative research group from McGill University (Montreal, QC, Canada), Harvard Medical School (Boston, MA), and Vanderbilt University (Nashville, TN) showed that KCC3 was responsible for a recessively inherited neurodegenerative disorder called agenesis of the corpus callosum with peripheral neuronopathy (ACCPN) or Andermann syndrome (60). This disorder is extremely rare with a prevalence rate of less than 1:1,000,000 individuals worldwide. Because of a founder effect, however, it is much more common in Quebec (Canada), especially between the Saguenay-Lac-Saint-Jean and Charlevoix regions near the Appalachian front where it affects ~1:2,000 live births (26, 39). Andermann syndrome, accordingly, is sometimes referred to as Charlevoix disease.

The neuropathy in ACCPN is sensorimotor in nature. It is therefore typically accompanied by areflexia, amyotrophy, and muscle weakness (5, 68). The corpus callosum is almost always atrophied as well, albeit to variable degrees (79). For this reason, at least in part, signs and symptoms may also include developmental delays, hypotonia, ataxia, decreased pain threshold, cognitive disabilities, and autistic-like behaviors. In addition to these abnormalities, many individuals with Andermann syndrome exhibit typical dysmorphic features such as hypertelorism, brachycephaly, a high-arched hard palate, syndactyly, and crossover toes (39).

The chromosomal region responsible for Andermann syndrome was first reported in 1996 by Casaubon et al. (18). This region, which was identified through linkage disequilibrium and genetic cartography analysis, corresponded to a 5-cm interval on chromosome 15 between markers D15S1040 and D15S118 (maximal LOD score: D15S971). Howard et al. (59) eventually uncovered the gene at cause by fine-mapping the same interval in 231 individuals from 50 different families and by screening *Kcc3*, a candidate gene within this interval, for pathogenic mutations. Through these studies, the region of interest was narrowed to ~1,000 kb between markers D15S1040 and ACTC (maximal LOD score: D15S1232) and four truncation mutations were identified in *Kcc3*. Eventually, the most common mutation in the French Canadian population was found to be c.2436delG; p.Thr813fs × 813, that is, a frameshift mutation in exon 18.

Howard et al. (60) obtained definitive proof that *Kcc3* was associated with Andermann syndrome by testing the functional consequences of p.Thr813fs × 813. Indeed, the truncated protein was found to be normally glycosylated and expressed at the cell surface of *X. laevis* oocytes, but it was completely inactive. In the mixed 129/Sv × C57BL/6 mouse background (Sv × BL6), along the same line, systemic (syst) homozygous replacement of exon 3 by a β-galactosidase-neomycin cassette flanked by stop codons on the 3′-end resulted in locomotor deficit and sensorimotor peripheral neuropathy as observed in the human disease. It was concluded then that KCC3 plays a critical role in central nervous system development and maintenance.

In a patient who was affected by early-onset and progressive peripheral motor neuropathy with axonal degeneration, Kahle et al. (64) have more recently identified a de novo heterozygous mutation in the *Kcc3* gene (c.2971A>G; p.T991A). In cultured fibroblasts isolated from this patient, the mutation was shown to activate the cotransporter constitutively by precluding its phosphorylation. In contrast to previous observations, however, phosphorylation of residue T_{991} in wild-type (WT) fibroblasts was enhanced under hypotonic condition (see Fig. 3*C* in Ref. 64, white boxes). Otherwise, the $KCC3^{T991A}$ mutant was found to be insensitive to WNK inhibitors in HEK-293 cells, and a syst-$Kcc3^{T991A/T991A}{}_{Sv \times BL6}$ mouse model generated by the same research group reproduced the patient's clinical, electrophysiological, and histopathological abnormalities.

Based on these observations, it was proposed that the mutation exerted its deleterious effect through cell shrinking-induced neuronal or axonal injury. In and of itself, however, the report of Kahle et al. revealed that a gain in KCC3 function could also elicit Andermann-like features in both mouse and human. Moreover, some of the structures affected by pathological changes in the syst-$Kcc3^{T991A/T991A}{}_{Sv \times BL6}$ model were the same as in the ${}_{H}$syst-$Kcc3^{\Delta 3^*/\Delta 3^*}{}_{Sv \times BL6}$ model. It was thus unclear why the gain in gene function failed to produce a mirror image phenotype. As an explanation for their findings, the research group suggested that the response of

certain cell types to either chronic shrinking or chronic swelling translated into analogous functional or lesional consequences in the nervous system.

Models of KCC3 Inactivation

Since the early 2000s, several mouse models of *Kcc3* inactivation were phenotyped to gain further insight regarding the role of this transporter in a variety of tissues or cell types and in a variety of physiological processes. In many studies, the mouse models exploited to these ends were the same as the one produced by Howard et al. (60) and by Boettger et al. (13). They will be called henceforth $_{H}$syst-*Kcc3*$^{\Delta 3^*/\Delta 3^*}{}_{Sv \times BL6}$ and $_{B}$syst-*Kcc3*$^{\Delta 3^*/\Delta 3^*}{}_{Sv \times BL6}$, respectively, using H to indicate that the model was from Howard, B that it was from Boettger, syst that gene inactivation was systemic, and Δ*x** that the mutated protein is devoid of exon *x* (in part or in full) and the subsequent amino acid sequence.

Table 3 lists the different *Kcc3*-null mouse models in question and provides a summary of the strategy used for gene inactivation along with some of the phenotypic features reported. Several of the abnormalities described and their physiological meaning will be presented at greater length below and in the light of additional observations. However, focus will be devoted to the phenotypes for which characterizations were more extensive. Note that most investigators have exploited the Sv × BL6 mixed mouse line as background to conduct their experiments. Garneau et al. (50), on the other hand, have recently opted for a pure C57BL/6J (BL6J) mouse line as a theoretically more suitable background to study the effect of *Kcc3* inactivation on cardiometabolic function (112, 118).

Central Nervous System

Much knowledge has been gained regarding the role of KCC3 in the central and peripheral nervous systems by identifying the gene responsible for Andermann syndrome. Substantial knowledge has also been gained by characterizing the *Kcc3*-null mouse models listed in Table 3. It will be summarized in this section along with a more precise account on the neural localization of KCC3. Despite the progress accomplished, however, it will appear obvious that uncertainty still remains as to the underlying pathological mechanisms and subpopulation of neurons or axons through which defective K^+-Cl^- cotransport accounts for the neurological manifestations of Andermann syndrome.

The $_{H}$syst-*Kcc3*$^{\Delta 3^*/\Delta 3^*}{}_{Sv \times BL6}$ model initially characterized (60) was found to exhibit weakness of the hindlimbs, loss of limb extension reflex during tail suspension, deficient sensory gating based on prepulse inhibition tests, and reduced exploratory movements. As for the associated pathological defects, they consisted of hypomyelination, axonal swelling, and fiber degeneration affecting peripheral nerves as observed in Anderman syndrome. Intriguingly, however, no such pathological defects were found in the brain or spinal cord of $_{H}$syst-*Kcc3*$^{\Delta 3^*/\Delta 3^*}{}_{Sv \times BL6}$ mice even if KCC3 was found to be normally expressed in hippocampus, pyramidal cells, cerebral cortex, Purkinje cells, and glial white matter tracts within the central nervous system of WT littermates. In this regard, KCC3 had also been detected by another research group in several structures of the central nervous system including white matter tracts along the corpus callosum and spinal cord (93).

Table 3. *Models of Kcc3 inactivation*

First Author	Howard	Boettger	Adragna	Rust	Byun	Jiao	Sun	Lucas	Shekarabi			Ding			Gameau
Journal	*Nat Genet* '02	*EMBO J* '03	*AEMB* '04	*Circ Res* '06; *JCI* '07	*NBD* '07	*Genomics* '08	*Glia* '10	*MCN* '12	*J Neurosci* '12			*BBR* '14			*PloS One* '16
Background	Sv × BL6	Sv × BL6	Sv × BL6	Sv × BL6†	Sv × BL6	C3H	Sv × BL6	Sv × BL6‡	Sv × BL6	Sv × BL6	Sv × BL6	Sv × BL6	Sv × BL6	Sv × BL6	BL6J
Mutation	$_{H}$Δ3*	$_{B}$Δ3*	$_{H}$Δ3*	$_{B}$Δ3*	$_{H}$Δ3*	Δ4*	$_{H}$Δ3*	$_{H}$Δ3*	Δ18*	Δ18*	Δ7*	Δ7*	Δ7*	Δ7*	Δ2*
Cells targeted	Syst	Syst	syst	syst	Syst	Syst	syst	Syst	*Syn1*	*Actb*	*Pvalb*	*Eno2*	*Scn10a*	*Dhh*	syst
Gait, posture	Abnormal	Abnormal	—	—	Abnormal	Abnormal	Abnormal	—	Abnormal	Abnormal	Abnormal	Normal	Normal	Normal	Abnormal
Locomotion	↓	↓	—	—	→	—	—	—	↔	↔	↓	Normal	Normal	Normal	—
Nociception	—	—	—	—	→	—	—	—	↔	↔	—	—	—	—	—
C. callosum	Normal	Normal	—	—	—	—	—	—	Hypoplasia	Hypoplasia	—	—	—	—	—
Neurons CNS	Normal	Degen	—	—	—	—	—	—	Normal	Normal	—	—	—	—	—
Axons CNS	Normal	Degen	—	—	—	—	—	—	Normal	Normal	—	—	—	—	—
Root ganglia	Normal	Degen	—	—	—	—	—	Degen	—	—	Degen	—	—	—	—
Axons PNS	Degen	Degen	—	—	Degen	—	Degen	—	Degen	Degen	—	—	—	—	—
Hearing	Normal?	↓	—	—	—	—	—	—	Normal	↓	—	—	—	—	—
MAP, mmHg	—	+18	+30	+13	—	—	—	—	−9	−14	—	—	—	—	+8
Weight, %	Normal	—	−12 (ns)	−8	—	—	—	—	—	—	—	—	—	—	−20
Diuresis, %	—	—	—	—	—	—	—	—	—	—	—	—	—	—	+60
Water intake, %	—	—	+22	—	—	—	—	—	—	—	—	—	—	—	+33
Chow intake, %	—	—	—	—	—	—	—	—	—	—	—	—	—	—	+68

At least 11 different *Kcc3*-null mouse models were generated since the early 2000s. The mixed 129/Sv × C57BL/6 mouse background (Sv × BL6) was used for most of them. The other backgrounds were: C3H × HeDiSnJ (C3H), and C57BL/6J (BL6J). H is used to indicate that the model was generated by Howard et al. (60), B, that it was generated by Boettger et al. (13). †Model was also produced in the SAD (syst-$Hbb^{SAD}{}_{BL6J \times CBA/J}$) background; ‡Swiss mice were used as WT controls. While the strains of Howard et al. and Boettger et al. look alike, the nucleotide cassette used for recombination was very different. Symbols used: −, data not provided; ↓, decreased; ↑, increased; Δ*x**, resulting protein devoid of exon *x* (in part or in full) and subsequent residues; degen, degenerescence; ns, nonsignificant; syst, systemic. Other abbreviations: AEMB, *Advances in Experimental Medicine and Biology*; BBR, *Behavioural Brain Research*; JCI, *Journal of Clinical Investigation*; MCN, *Molecular and Cellular Neuroscience*; NBD, *Neurobiology of Disease*.

In 2003, Boettger et al. (13) reported the neurological phenotype of their own $_{B}$syst-*Kcc3*$^{\Delta 3*/\Delta 3*}{}_{Sv \times BL6}$ model. They observed posture and motor defects as well, but in addition to these abnormalities, epileptic thresholds under flurothyl inhalation were decreased concomitantly. As for the tissues affected by degenerative changes, they not only included the peripheral nervous system, but also white matter tracts in the brain and spinal cord, various regions of the hippocampus and cerebellum as well spinal root ganglia. Otherwise, refined localization studies were partly consistent with those of Howard et al. (60) but failed to reveal the presence of KCC3 in glial white matter tracts along the corpus callosum and spinal cord. In fact, KCC3 was detected more specifically within the synaptic domains of brain and spinal cord neurons.

Such differences in anatomical phenotypes and sites of KCC3 expression between the $_{H}$syst-*Kcc3*$^{\Delta 3*/\Delta 3*}{}_{Sv \times BL6}$ and $_{B}$syst-*Kcc3*$^{\Delta 3*/\Delta 3*}{}_{Sv \times BL6}$ mouse models could be due to a number of factors. For instance, it is possible that the Sv × BL6 backgrounds used for *Kcc3* inactivation were not exactly the same, especially if they were not generation-matched during the studies. It is also possible that the truncated KCC3 protein exerted a number of divergent cellular effects between the genotypes in not being identical either. Lastly, the approaches and antibodies used by each of the research groups in various characterizations differed as well so that inconsistencies were to be expected from the outset.

Based on their observations, Boettger et al. (13) suggested nonetheless that the absence of KCC3 in glial cells played no pathophysiological role in neuronal or axonal degeneration as previously suggested by other research groups (60). They suggested that this abnormality was due instead to chronic swelling of KCC3-deficient neurons. To this effect, they showed that primary cultures of hippocampal neurons derived from $_{B}$syst-*Kcc3*$^{\Delta 3*/\Delta 3*}{}_{Sv \times BL6}$ mice exhibited an abnormal regulatory volume decrease (RVD) response. They also showed that Purkinje cells analyzed in parasagittal brain slices derived from these mice exhibited increased $[Cl^-]_i$ along with γ-aminobutyric acid (GABA)-induced hyperpolarization. Lucas et al. (76) later demonstrated that *Kcc3* inactivation caused $[Cl^-]_i$ to increase in other types of neurons, that is, in primary cultures of dorsal ganglia cells derived from the $_{H}$syst-*Kcc3*$^{\Delta 3*/\Delta 3*}$ mouse model.

Two research groups have recently used the $_{H}$syst-*Kcc3*$^{\Delta 3*/\Delta 3*}{}_{Sv \times BL6}$ model to investigate the role of KCC3 in peripheral axons (16, 116). One group (Byun and Delpire) observed that the sciatic nerve of these mice was affected by periaxonal fluid accumulation at an early age followed by axonal and myelin degeneration at an older age. Yet, interestingly, the sciatic nerve of WT littermates only expressed KCC3 at an early age. They concluded that *Kcc3* inactivation caused sciatic nerve damage through an initial phase of axonal hydrops due to loss of K^+-Cl^- cotransport in situ. Another group (Sun et al.) found that KCC3 was expressed in sciatic nodal segments and that loss of K^+-Cl^- cotransport at this site led in vivo conduction velocity to decrease. In this study, the mutant mouse model was exploited as is or WT mice were injected in their sciatic nerve with inhibitors of KCC3, the main KCC isoform in peripheral axons. It was concluded that KCC3 played an important role in action potential propagation peripherally.

In 2012, Shekarabi et al. (104) examined a neuron-specific *Kcc3*-null model in which gene ablation was limited to *Syn1*-expressing neurons (*Syn1-Kcc3*$^{\Delta 18*/\Delta 18*}{}_{Sv \times BL6}$) and compared it to a model in which ablation was more generalized, that is, affected β-actin-expressing cells (*Actb-Kcc3*$^{\Delta 18*/\Delta 18*}{}_{Sv \times BL6}$). Both genotypes were found to be affected by a hyperactive rather than hypoactive locomotor phenotype, corpus callosum atrophy and severe sciatic axonopathy with decreased sensitivity to inflammatory pain responses, but no signs of abnormal corpus callosum development during embryogenesis. From these observations, which were in contrast with those of previous studies (35, 60), Shekarabi et al. concluded that *Kcc3* deletion in neurons was sufficient to cause the observed abnormalities and that KCC3 was not involved in axonal growth during development but axonal maintenance during life.

To identify the population of cells through which defective KCC3 activity causes neurological manifestations, Ding et al. (35) reported the phenotypes of four additional neuron-specific *Kcc3*$^{\Delta 7*/\Delta 7*}{}_{Sv \times BL6}$ models. Mice were inactivated for *Kcc3* in parvalbumin (*Pvalb*)-, enolase-2 (*Eno2*)-, sodium channel $Na_v1.8$ (*Scn10a*)-, or desert hedgehog (*Dhh*)-expressing neurons, that is, in fast-spiking GABAergic interneurons, mature neurons, nociceptive neurons, and Schwann cells, respectively. Neurological abnormalities were only observed in *Pvalb-Kcc3*$^{\Delta 7*/\Delta 7*}{}_{Sv \times BL6}$ mice and were accompanied by vacuolization of proprioceptive type 1A fibers in dorsal root ganglia. Intriguingly, inactivation driven by *Eno2* produced no defects even if this gene is expressed in the same cell types as *Syn1* (11, 66, 78, 117, 127). Background- or mutation-dependent effects could have thus accounted once again for a number of discrepancies. In addition, it is not clear that the degree of *Kcc3* inactivation was equivalent in all cell types between the two models.

Growth, Adiposity, and Metabolism

Five of the *Kcc3*-null mouse models generated during the last 15 years have been reported to be affected by low body weight with or without reduced size at adult age (see Table 3). This trait was initially described in 2004 by Adragna et al. (1) in the $_{H}$syst-*Kcc3*$^{\Delta 3*/\Delta 3*}{}_{Sv \times BL6}$ mouse model. Based on the available literature, however, it was found to be most pronounced in the syst-*Kcc3*$^{\Delta 2*/\Delta 2*}{}_{BL6J}$ model of Garneau et al. (50), that is, in a background generally considered as more suitable to study the effect of various interventions on cardiometabolic function. The data generated by this research group are summarized in Table 4. Striking differences were seen between mutant and WT animals at 5 to 7 months of age. In particular, body weight was 1.2-fold lower and gonadal fat weight 4.5-fold lower. The phenotype observed was therefore one of marked leanness.

Subsequent to their initial observations, Garneau et al. (50) conducted a series of additional experiments to understand the mechanisms of low adiposity in the syst-*Kcc3*$^{\Delta 2*/\Delta 2*}{}_{BL6J}$ model and its potential consequence on metabolism and energy allocation. They found that in comparison to WT littermates, serum catecholamine levels were not altered substantially, chow intake was unexpectedly much higher, serum profile of adipokines was healthier, and glucose utilization was probably enhanced (see examples of data obtained in Table 4). Among different possibilities, these findings suggest that KCC3 could

play an important role in energy homeostasis or adipocyte function and, therefore, in obesity development and cardiometabolic dysfunction. They also suggest that *Kcc3* inactivation in certain tissues or cell types could exert beneficial effects.

At this stage, whether low adiposity occurred because of deficient K^+-Cl^- cotransport in adipocytes or in the nervous system needs to be clarified. In this regard, the *Syn1-Kcc3*$^{\Delta 18*/\Delta 18*}{}_{Sv \times BL6}$ mouse model of Shekarabi et al. (104) was also found to exhibit a significant decrease in body weight at 2 months even if gene inactivation in these mice was theoretically limited to neurons. As stated earlier, however, the *Syn1-Kcc3*$^{\Delta 18*/\Delta 18*}{}_{Sv \times BL6}$ model was affected much more severely than the *Eno2-Kcc3*$^{\Delta 7*/\Delta 7*}{}_{Sv \times BL6}$ model of Ding et al. (35) while *Syn1* and *Eno2* are expressed in the same neurons. Hence, one cannot exclude that in the study of Shekarabi et al., *Syn1*-driven *Kcc3* inactivation affected nonneuronal or nonextraneural cell types through leaky *Syn1* expression. One cannot exclude either that in the study of Garneau et al. (50), some of the observed metabolic defects also developed through unique, background-specific mechanisms.

Table 4. *Cardiometabolic phenotype of syst-Kcc3*$^{\Delta 2*/\Delta 2*}{}_{BL6J}$ *mouse model*

Determinations	*Kcc3*$^{+/+}$	*Kcc3*$^{-/-}$
A) Hemodynamics (change relative to WT)		
Systolic blood pressure, mmHg	—	−0.2 ± 1.8
Mean arterial pressure, mmHg	—	+8.1 ± 3.8
Diastolic blood pressure, mmHg	—	+11.2 ± 4.3
Pulse pressure, mmHg	—	−9.4 ± 2.0
Heart rate, beats/min	—	−62 ± 12
B) Cardiac weight		
Absolute weight, mg	141.9 ± 2.9	149.1 ± 2.7
Absolute weight normalized to TBW, %	0.391 ± 0.010	0.510 ± 0.007
C) Echocardiographic measurements		
LV end-diastolic diameter, mm	3.85 ± 0.05	4.18 ± 0.05
LV weight/tibial length, g/mm	5.24 ± 0.30	6.32 ± 0.25
LV weight/TBW, %	0.408 ± 0.026	0.544 ± 0.025
D) Metabolic features		
Adult TBW, g	36.6 ± 1.1	29.3 ± 0.5
Gonadal fat normalized to TBW, %	4.85 ± 0.39	1.51 ± 0.27
Adiponectine, *n*-fold change relative to WT	1.00 ± 0.20	3.68 ± 1.02*
Fasting glycemia, mmol/l	8.78 ± 0.23	6.16 ± 0.13*
E) Other parameters		
Daily chow intake, g	2.2 ± 0.2	3.7 ± 0.1
Daily water intake, ml	3.0 ± 0.3	4.0 ± 0.1
Hourly diuresis, μl	31.4 ± 3.6	50.2 ± 3.2
Urine osmolality, osmol/kg	1.99 ± 0.15	1.99 ± 0.11

Data are expressed as means ± SE. *A*) Hemodynamic parameters were obtained through sphygmomanometric measurements (n = 4–6 mice). *B*) Cardiac weight (n = 29–32). TBW, total body weight. *C*) Echocardiographic measurements (n = 8). LV, left venricular. *D*) Metabolic features (n = 16 for TBW and gonadal fat weight, 4 for adiponectine, 9 for glycemia). *E*) Other parameters (n = 5–11 mice). Statistical analyses were carried out through Student's *t*-tests or Wilcoxon's rank-sum tests. The data presented are from Garneau et al. (50) and from subsequent unpublished experiments by the same research group (*). Except for systolic blood pressure and urine osmolality, all of the data shown are statistically different between *Kcc3*-null mice and wild-type littermates. Note that blood pressure measurements were also reported by other research groups in the Sv × BL6 mouse background. They are partially summarized in Table 3 and presented in greater detail under section *Cardiovascular Function.* Otherwise, most of the measurements shown in the Table have only been reported in the BL6J background.

Cardiovascular Function

Three of the *Kcc3*-null mouse models produced were found to manifest arterial hypertension in addition to the other traits. Boettger et al. (13) were the first research group to report this abnormality. In more specific terms, they found that light phase mean arterial blood pressure (MAP) measured in their $_{B}$syst-*Kcc3*$^{\Delta 3*/\Delta 3*}{}_{Sv \times BL6}$ model through femoral artery catheterization was 18 mmHg higher compared with WT mice. Animals were 3 to 5 months of age and tethered during the measurements. Adragna et al. (1) later reported the same abnormality in the $_{H}$syst-*Kcc3*$^{\Delta 3*/\Delta 3*}{}_{Sv \times BL6}$ model of Howard et al. (60). In their study, indeed, both light and dark phase MAPs measured by telemetry through carotid artery catheterization were found to be 30 mmHg higher compared with WT mice. Animals were 5 to 6 months of age during the experiments.

The mechanisms of high blood pressure were explored a few years later by Rust et al. (100) in the $_{B}$syst-*Kcc3*$^{\Delta 3*/\Delta 3*}{}_{Sv \times BL6}$ model. Animals were 3 to 4 months of age during the studies. It was found that dark phase MAP measured through femoral artery catheterization in tethered *Kcc3*-null mice and WT littermates was equally reactive to α_1-adrenoreceptor stimulation, β_1-adrenoreceptor inhibition, and exogenous nitric oxide administration, but more sensitive in the null mice to ganglionic and α_2-adrenoreceptor inhibition. It was found, in addition, that third-order saphenous arteries isolated from the null mice and their WT littermates exhibited the same reactive phenotypes in response to intravascular pressure, α_1-adrenoreceptor stimulation, exogenous nitric oxide administration, or Ca^{2+}-activated Cl^- channel (CACC) inhibition. It was therefore concluded that *Kcc3* inactivation led to arterial hypertension through neurogenic mechanisms.

In the study of Rust et al. (100), it is noteworthy that the saphenous arteries of $_{B}$syst-*Kcc3*$^{\Delta 2*/\Delta 2*}{}_{Sv \times BL6}$ mice were hypertrophied and that their $[Cl^-]_i$ was also increased compared with WT littermates. Other mechanisms could have thus contributed to the cardiovascular phenotype reported by this research group such as decreased K^+-Cl^- cotransport in VSMCs where KCC3 is known to be expressed (33, 50, 100). To this effect, isolated arterial vessels inactivated for *Nkcc1* have been found to display decreased Cl^- content as well as blunted responses to vasoconstrictive agents (4, 85), implying that KCC3 and NKCC1 could play reciprocal functional roles in the arterial wall. As already stated, importantly, the mixed Sv × BL6 background is perhaps not ideal to study the cardiovascular system of mouse models (112).

Garneau et al. (50) have recently reassessed the effect of *Kcc3* inactivation on cardiovascular function in their BL6J model to determine whether vasculogenic mechanisms could be at play. Animals were 2 to 3 months of age during the experiments and their blood pressures were measured by sphygmomanometry. As shown in Table 4, these studies led to the identification of previously unreported features. Compared with WT mice, for instance, pulse pressure and heart rate were lower in the null mice, but diastolic blood pressure, left ventricular mass, and urine output were higher. In addition, thoracic aortas isolated from $_{syst}$*Kcc3*$^{\Delta 2*/\Delta 2*}{}_{BL6J}$ mice exhibited decreased wall thickness and reactivity to α_1-adrenoreceptor stimulation (Fig. 6). Given that they were characterized while denervated and that WT thoracic aortas were found to express KCC3, Garneau et al. concluded that reduction of K^+-Cl^-

cotransport in the cardiovascular tree could have accounted for a number of the observed abnormalities.

Hearing

Epithelial ion transport systems in the organ of Corti play a crucial role in vestibulocochlear function and development. It is thus not surprising that three CCC family members have been detected in this structure, namely, KCC3, KCC4, and NKCC1 (12, 13, 31, 37, 41, 67, 104, 122). While KCC3 is expressed in the stria vascularis (type I and III fibrocytes), supporting inner hair cells (sIHCs), Deiters' supporting outer hair cells (sOHCs), and other supporting cells within the inner hear of rodents, KCC4 and NKCC1 are expressed more restrictively, that is, in sIHCs and sOHCs for the Na^+-independent CCC and the stria vascularis (type II fibrocytes and marginal cells) for the Na^+-dependent CCC.

Based on their localization and as illustrated in Fig. 7, the role of KCC3, KCC4 and NKCC1 in the inner ear is probably to sustain K^+ recycling after its entry in IHCs and OHCs, that is, to promote K^+ movement from these cells to the perilymph through supporting cells (KCC3 and KCC4) and its movement from the perilymph to the endolymph through the stria vascularis (NKCC1 and KCC3). According to certain investigators, the role of these CCCs could also be to buffer $[K^+]_e$ or to regulate the volume of various cell types within the inner ear (12, 122). Another possibility is that the auditory CCCs could play either of these roles in response to specific environmental cues.

In their $_{B}$syst-*Kcc3*$^{\Delta 3*/\Delta 3*}{}_{Sv \times BL6}$ model, Boettger et al. (13) found that hearing was normal at birth, but that deafness progressed slowly thereafter during the first year of life and that this anomaly was accompanied by degenerative changes of several structures and cell rarefaction within the inner ear. As expected, type II fibrocytes were spared even in the older animals. Intriguingly, inactivation of *Kcc4* in another study by Boettger et *al.* (12), apparently led to more rapid hearing loss and degenerative changes even though its expression in the organ of Corti is more restricted and is redundant with that of *Kcc3*. Perhaps the effect of interrupting the perilymph-to-endolymph and endolymph-to-perilymph K^+ recycling axes together is more deleterious than interrupting only one of them.

In more recent studies, Shekarabi et al. (104) also characterized the auditory system of their two animal models, that is, of *Actb-Kcc3*$^{\Delta 18*/\Delta 18*}{}_{Sv \times BL6}$ and *Syn1-Kcc3*$^{\Delta 18*/\Delta 18*}{}_{Sv \times BL6}$ mice, but through a combination of functional studies and diffusion magnetic resonance imaging of the auditory cortex. They observed that acoustic tests were abnormal in the systemic null mouse, but not in the neurospecific one, and that the auditory cortex was atrophied in the latter, but not in the former. They therefore concluded that auditory dysfunction through systemic *Kcc3* inactivation originated from defective K^+-Cl^- cotransport in nonneuronal cells. It should be noted,

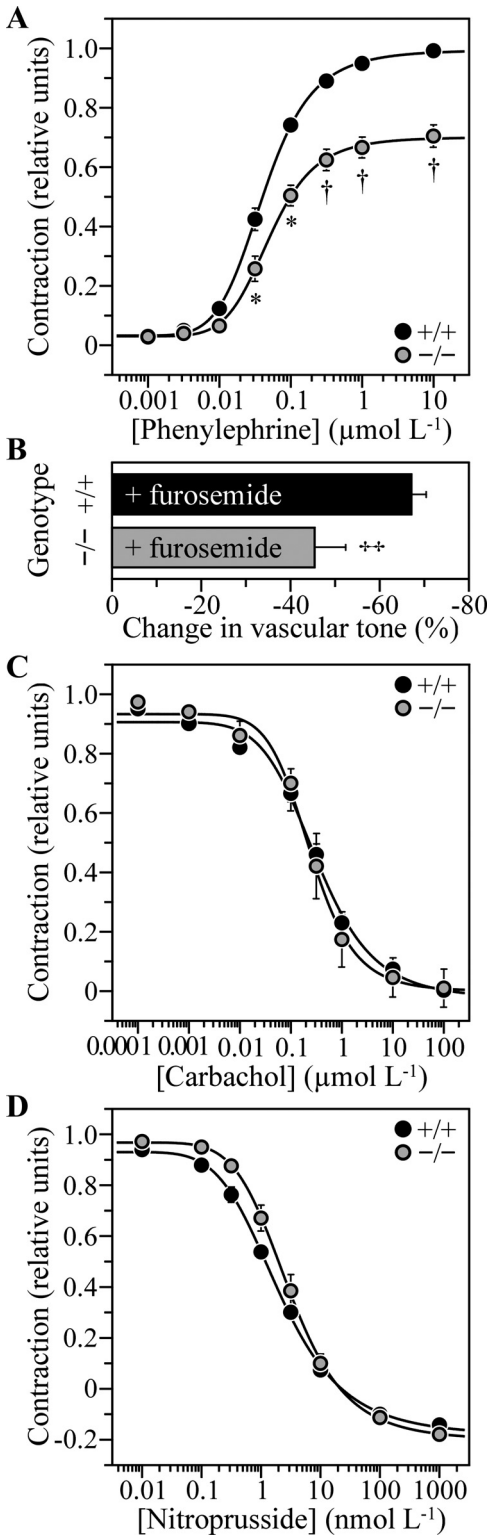

Fig. 6. Reactivity of isolated thoracic aorta cut into 2-mm segments. *A*: effect of phenylephrine hydrochloride shown as normalized isometric force development. Data expressed as means ± SE are from 6 mice among 6 experiments. * and † indicate that the data are statistically different between *Kcc3*-null mice and wild-type littermates at $P < 0.05$ and $P < 0.01$, respectively. *B*: effect of furosemide on precontracted aortic segments shown as inhibitor-induced changes in aortic tone. Data expressed as means ± SE are from 4 mice among 4 experiments. ‡ indicates that the mean is statistically different compared with WT littermates. *C*: effect of carbamoyl chloride on precontracted aortic segments shown as normalized isometric force development. Data expressed as means ± SE are from 5 mice among 5 experiments. *D*: effect of Na^+ nitroprusside on precontracted aortic segments shown as normalized isometric force development. Data expressed as means ± SE are from 5 mice among 5 experiments. The data and figure presented are from Garneau et al. (50).

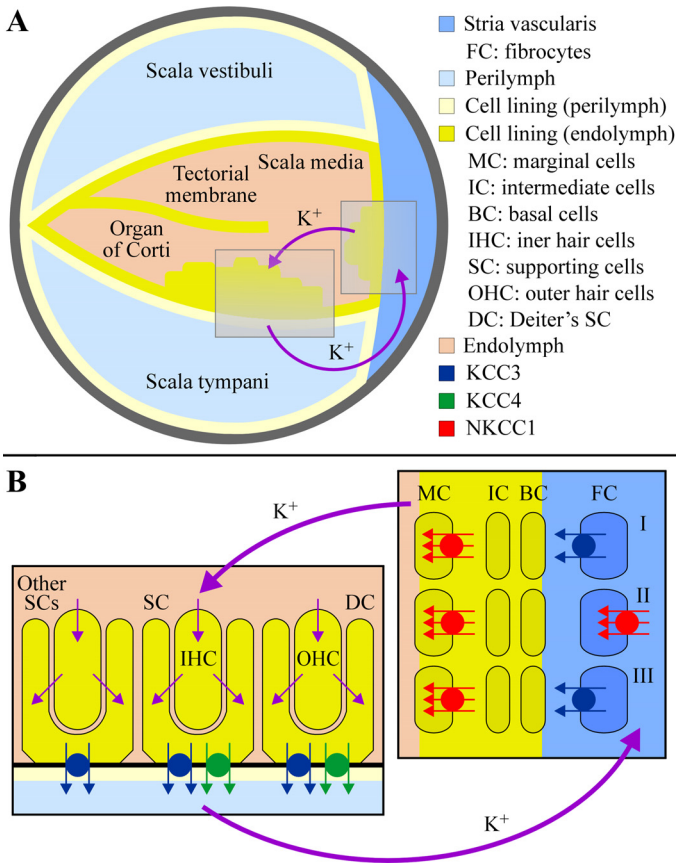

Fig. 7. KCC3-dependent ion transport in the inner ear. *A*: cross section of the cochlea with its main compartments, that is, the scala vestibuli, scala media, scala tympani, and stria vascularis. *B*: magnification of the regions shown by the boxes in *A* with the cells types where the CCCs are expressed. The precise localization of each isoform within these cell types has not been definitively established. Color codes and abbreviations used are as indicated in the accompanying legend.

however, that the organ of Corti was not subjected to histological analyses in this study.

Renal Function

According to the EST database and Northern blot analyses, KCC3 is clearly expressed in the kidney of rat and human (57, 88, 96), and according to immunofluorescence studies, it is confined to the basolateral membrane of proximal renal tubular cells along the S1, S2, and S3 segments (13, 80, 84). In two different reports (84, 93), Northern blot analyses also showed that the KCC3B splice variant was more abundant in mouse kidney than the KCC3A variant. At the same time, the probes used to detect each of the transcripts were not the same (84, 93), and in one of the reports (84), concomitant reverse transcriptase (RT)-PCR studies did not corroborate these findings. Melo et al. (80) have more recently found that KCC3 was upregulated in the kidney of WT rodents during hyperglycemia. However, the splice variant at cause and its specific renal localization within the renal epithelium were not determined.

Because of its renal localization and transport properties, one would expect KCC3 to play an important role in solute reabsorption by the proximal nephron. One would also expect both KCC3A and KCC3B to be involved in this process given that each of them has been found to be functional in *X. laevis* oocytes (84). Yet, the study by Melo et al. (80) convincingly showed that carrier expression was not upregulated in rodents through salt deprivation. It was not upregulated either during chronic acidosis even though KCC3 activity is known to be highly pH-sensitive (10). While, as just reported, hyperglycemia did augment carrier abundance in the renal cortex, the underlying mechanisms were not explored experimentally. Among other possibilities, an increase in tubular flow due to prolonged glycosuria could have accounted for these observations given that it has been shown to alter the activity of other ion transport systems as well (17).

In earlier studies, two research groups have convincingly demonstrated the presence of a K^+-Cl^- cotransport system in the basolateral membrane of isolated rabbit proximal tubules (6, 103). However, it was not possible to determine the exact isoforms at play given that their molecular identity was still unknown at the time. In retrospect, KCC3 was certainly a good candidate, all the more so that the K^+-Cl^- cotransport system characterized in one of these studies (6) was found to be enhanced in the presence of glucose. Importantly, however, KCC4 could also play an important role in solute reabsorption by the proximal nephron given that two research groups have detected its presence at the basolateral membrane of this tubular segment (12, 119).

The animal models of *Kcc3* inactivation have provided additional indication that KCC3 could play a role in water and salt handling by the proximal nephron. For instance, Boettger et al. (13) showed strong expression of KCC3 at the basolateral membrane of proximal tubular cells in WT mice, and loss of expression in $_{B}$syst-Kcc3$^{\Delta 3*/\Delta 3*}{}_{Sv \times BL6}$ littermates. Along the same line, Wang et al. (123) observed that the $_{H}$syst-Kcc3$^{\Delta 3*/\Delta 3*}{}_{Sv \times BL6}$ model was affected by higher urinary output compared with WT mice and lower fluid reabsorption in their proximal nephron. Importantly, however, fluid intake was also increase in the mutant mice. Garneau et al. (50) have found more recently that their syst-*Kcc3*$^{\Delta 2*/\Delta 2*}{}_{BL6J}$ mice presented similar abnormalities and that, in addition, they ingested higher daily amounts of chow compared with WT mice. As it stands, hence, it cannot be excluded that the renal phenotype of these *Kcc3*-null models was dietary in origin.

Red Blood Cells

As mentioned earlier, erythrocytes have long been known to display robust KCC activity. Although they express five different KCC splice variants (21, 70, 99), that is, KCC1A, KCC1B, KCC3A, KCC3B, and KCC4, K^+-Cl^- cotransport activity in these cells is primarily accounted for by KCC3A. In particular, Western blot analyses and qPCR studies carried out by Pan et al. (90) have shown that the other variants were expressed at much lower levels in human and mouse erythrocytes. Along the same line, Rust et al. (100) have shown that the erythrocytes of $_{B}$syst-*Kcc3*$^{\Delta 3*/\Delta 3*}{}_{Sv \times BL6}$ mice exhibited much lower K^+-Cl^- cotransport activity than those of a model called syst-*Kcc1*$^{\Delta 4*/\Delta 4*}{}_{Sv \times BL6}$ generated more recently by the research group itself.

Many investigators have now established that the presence of KCC3 at the cell surface of erythrocytes is of central importance in the pathophysiology of sickle cell anemia (19, 21, 73, 99), an inherited hemoglobinopathy that affects mil-

lions of individuals worldwide. In this disorder, the mutated hemoglobin (Hb) forms large insoluble polymers that alter the shape of erythrocytes both directly and through cytoskeletal rearrangements. In this setting, but through unknown mechanisms, K^+-Cl^- cotransport is enhanced so that erythrocytes are partially dehydrated due to secondary osmotic efflux of water. From these additional changes, the abnormal shape and increased rigidity of erythrocytes are accentuated and the abnormal Hb is concentrated excessively so that it polymerizes even more easily.

Rust et al. (99) have confirmed more definitively the role of KCC3 in the pathophysiology of sickle cell anemia by studying the effect of *Kcc3* inactivation in a transgenic mouse background of hypersickling human HbS overexpression called SAD (or syst-$Hbb^{SAD}{}_{BL6J \times CBA/J}$). They observed that the erythrocytes of syst-$Kcc3^{\Delta 3*/\Delta 3*}{}_{SAD}$ mice were not as dense and not as small in volume as those of syst-$Kcc3^{+/+}{}_{SAD}$ mice. However, the abnormal cells were morphologically similar between the two models and the densest ones were not rescued through *Kcc3* inactivation, suggesting that other transport proteins such as KCC1 and Ca^{2+}-activated K^+ channel 4 (KCNN4) could have contributed to the loss of cytosolic water. In this regard, Rust et al. (99) also observed that dual inactivation of *Kcc1* and *Kcc3* in the SAD background led mean corpuscular volume to increase further, confirming that KCC1 does play an accessory role in the pathophysiology of sickle cell anemia.

White Blood Cells

KCC3 has been found to play additional roles in blood such as regulating the activity of neutrophils through its Cl^- transport function (43, 115). In this cell type, pathogens are internalized from the cell surface into phagosomes where they are killed through chemical digestion. One of the compounds involved, hypochlorite, is generated in situ from hydrogen peroxide and Cl^-. The first substrate is derived from superoxide, itself generated by nicotinamide adenine dinucleotide phosphate (NADPH) oxidase, and the second substrate is provided by the cytosol where, in neutrophils, $[Cl^-]_i$ is especially high. Dedicated Cl^- transport systems must therefore be present at the surface of phagosomes in order for this organelle to dispose of all of the substrates required for hypochlorite synthesis.

Sun et al. (115) were the first research group to demonstrate the dependence of phagosomal function on KCC3. Indeed, they found that neutrophils isolated from WT mice were less prone to activation in the presence of KCC inhibitors, that is, superoxide production was lower, and so were the membrane recruitment and phosphorylation state of oxidases such as neutrophil cytosolic factors 1 and 4. They found more importantly that $_H$syst-$Kcc3^{\Delta 3*/\Delta 3*}{}_{Sv \times BL6}$ mice infected with *Staphylococcus aureus* suffered higher mortality rates as well as lower bacterial clearance compared with WT littermates and that their neutrophils were also less prone to activation. In light of these findings, and based on concomitant localization studies, Sun et al. concluded that KCC3 sustains the bactericidal activity of phagosomes by providing them with an inward pathway for Cl^- movement during neutrophil activation.

CONCLUSIONS

Through this review, it was shown that KCC3 is involved in a variety of physiological processes. It was also shown that this transport system is likely to play an essential, nonredundant role in many cell types within the central and peripheral nervous systems, inner ear, cardiovascular tissue and blood. Additional processes for which KCC3 could be of importance, but were not discussed through this review, include spermatozoal subsistence (65), catecholamine release by adrenal medullary chromaffin cells (50), and glucagon secretion by pancreatic α-cells (24). As alluded to in *Regulation of KCC3 and of Other Subfamily Members*, they also include normal as well as abnormal cell growth and proliferation. In fact, the role of KCC3 in cancer development and invasiveness has now become the object of an emerging literature of potentially high future impact (20, 46, 106).

Although the animal models of *Kcc3* inactivation have revealed physiologically and pathophysiologically informative, they have also led to conflicting results due perhaps to differences in the animal backgrounds, targeting strategies and experimental approaches exploited. In particular, the mechanisms of axonal degeneration in ACCPN are still largely unknown and so is the subpopulation of neurons that are adversely affected through loss of K^+-Cl^- cotransport. Additionally, protein expression was not completely ablated in some of the cell-specific *Kcc3*-null mouse models generated and it was even partially ablated in one study (104) through mere recombination of a flox cassette at the *Kcc3* locus, that is, in Cre^- $Kcc3^{\Delta 18*/\Delta 18*}{}_{Sv \times BL6}$ mice.

There are many additional uncertainties besides those pertaining to the physiological roles of KCC3 in the nervous system and other tissues. For instance, the number of ion transport sites that are required for translocation is still unknown and the mechanisms by which K^+-Cl^- cotransport is regulated remain poorly understood. Likewise, the deleterious effects of *Kcc3* inactivation have generally been ascribed to perturbed RVD responses and yet this transporter is known to affect the intracellular and extracellular concentrations of many solutes either directly or through other transport systems. Although the "KCC3 story" has been unfolding before our eyes for almost four decades, its final chapter will certainly not be written any time soon.

DISCLOSURES

No conflicts of interest, financial or otherwise, are declared by the authors.

AUTHOR CONTRIBUTIONS

A.P.G., R.F.-C., J.L.L., and P.I. conceived and designed research; A.P.G. and R.F.-C. performed experiments; A.P.G., R.F.-C., J.L.L., and P.I. analyzed data; A.P.G., R.F.-C., J.L.L., and P.I. interpreted results of experiments; A.P.G., A.-A.M., R.F.-C., and P.I. prepared figures; A.P.G., A.-A.M., F.M.-W., and P.I. drafted manuscript; A.P.G., A.-A.M., R.F.-C., F.M.-W., J.L.L., and P.I. edited and revised manuscript; A.P.G., A.-A.M., R.F.-C., F.M.-W., J.L.L., and P.I. approved final version of manuscript.

REFERENCES

1. **Adragna NC, Chen Y, Delpire E, Lauf PK, Morris M.** Hypertension in K-Cl cotransporter-3 knockout mice. *Adv Exp Med Biol* 559: 379–385, 2004. doi:10.1007/0-387-23752-6_35.
2. **Adragna NC, Di Fulvio M, Lauf PK.** Regulation of K-Cl cotransport: from function to genes. *J Membr Biol* 201: 109–137, 2004. doi:10.1007/s00232-004-0695-6.

3. **Agalakova NI, Gusev GP.** Effects of phorbol 12-myristate 13-acetate on potassium transport in the red blood cells of frog *Rana temporaria*. *J Comp Physiol B* 179: 443–450, 2009. doi:10.1007/s00360-008-0324-2.
4. **Akar F, Skinner E, Klein JD, Jena M, Paul RJ, O'Neill WC.** Vasoconstrictors and nitrovasodilators reciprocally regulate the Na^+-K^+-$2Cl^-$ cotransporter in rat aorta. *Am J Physiol Cell Physiol* 276: C1383–C1390, 1999.
5. **Andermann E, Andermann F, Joubert M, Melançon D, Karpati G, Carpenter S.** Three familial midline malformtion syndromes of the central nervous system: agenesis of the corpus callosum and anterior horn-cell disease; agenesis of cerebellar vermis; and atrophy of the cerebellar vermis. *Birth Defects Orig Artic Ser* 11: 269–293, 1975.
6. **Avison MJ, Gullans SR, Ogino T, Giebisch G.** Na^+ and K^+ fluxes stimulated by Na^+-coupled glucose transport: evidence for a Ba^{2+}-insensitive K^+ efflux pathway in rabbit proximal tubules. *J Membr Biol* 105: 197–205, 1988. doi:10.1007/BF01870997.
7. **Bergeron MJ, Boggavarapu R, Meury M, Ucurum Z, Caron L, Isenring P, Hediger MA, Fotiadis D.** Frog oocytes to unveil the structure and supramolecular organization of human transport proteins. *PLoS One* 6: e21901, 2011. doi:10.1371/journal.pone.0021901.
8. **Bergeron MJ, Frenette-Cotton R, Carpentier GA, Simard MG, Caron L, Isenring P.** Phosphoregulation of K^+-Cl^- cotransporter 4 during changes in intracellular Cl^- and cell volume. *J Cell Physiol* 219: 787–796, 2009. doi:10.1002/jcp.21725.
9. **Bergeron MJ, Gagnon E, Caron L, Isenring P.** Identification of key functional domains in the C terminus of the K^+-Cl^- cotransporters. *J Biol Chem* 281: 15959–15969, 2006. doi:10.1074/jbc.M600015200.
10. **Bergeron MJ, Gagnon E, Wallendorff B, Lapointe JY, Isenring P.** Ammonium transport and pH regulation by K^+-Cl^- cotransporters. *Am J Physiol Renal Physiol* 285: F68–F78, 2003. doi:10.1152/ajprenal.00032.2003.
11. **Bock E, Dissing J.** Demonstration of enolase activity connected to the brain-specific protein 14-3-2. *Scand J Immunol* 4: 31–36, 1975. doi:10.1111/j.1365-3083.1975.tb03806.x.
12. **Boettger T, Hübner CA, Maier H, Rust MB, Beck FX, Jentsch TJ.** Deafness and renal tubular acidosis in mice lacking the K-Cl co-transporter Kcc4. *Nature* 416: 874–878, 2002. doi:10.1038/416874a.
13. **Boettger T, Rust MB, Maier H, Seidenbecher T, Schweizer M, Keating DJ, Faulhaber J, Ehmke H, Pfeffer C, Scheel O, Lemcke B, Horst J, Leuwer R, Pape HC, Völkl H, Hübner CA, Jentsch TJ.** Loss of K-Cl co-transporter KCC3 causes deafness, neurodegeneration and reduced seizure threshold. *EMBO J* 22: 5422–5434, 2003. doi:10.1093/emboj/cdg519.
14. **Brazy PC, Gunn RB.** Furosemide inhibition of chloride transport in human red blood cells. *J Gen Physiol* 68: 583–599, 1976. doi:10.1085/jgp.68.6.583.
15. **Brunet GM, Gagnon E, Simard CF, Daigle ND, Caron L, Noël M, Lefoll MH, Bergeron MJ, Isenring P.** Novel insights regarding the operational characteristics and teleological purpose of the renal Na^+-K^+-Cl2 cotransporter (NKCC2s) splice variants. *J Gen Physiol* 126: 325–337, 2005. doi:10.1085/jgp.200509334.
16. **Byun N, Delpire E.** Axonal and periaxonal swelling precede peripheral neurodegeneration in KCC3 knockout mice. *Neurobiol Dis* 28: 39–51, 2007. doi:10.1016/j.nbd.2007.06.014.
17. **Capasso G, Mollica F, Saviano C, De Santo NG.** Tubule effects of glomerular hyperfiltration: an integrated view. *Semin Nephrol* 15: 419–425, 1995.
18. **Casaubon LK, Melanson M, Lopes-Cendes I, Marineau C, Andermann E, Andermann F, Weissenbach J, Prévost C, Bouchard JP, Mathieu J, Rouleau GA.** The gene responsible for a severe form of peripheral neuropathy and agenesis of the corpus callosum maps to chromosome 15q. *Am J Hum Genet* 58: 28–34, 1996.
19. **Casula S, Shmukler BE, Wilhelm S, Stuart-Tilley AK, Su W, Chernova MN, Brugnara C, Alper SL.** A dominant negative mutant of the KCC1 K-Cl cotransporter: both N- and C-terminal cytoplasmic domains are required for K-Cl cotransport activity. *J Biol Chem* 276: 41870–41878, 2001. doi:10.1074/jbc.M107155200.
20. **Chiu MH, Liu HS, Wu YH, Shen MR, Chou CY.** SPAK mediates KCC3-enhanced cervical cancer tumorigenesis. *FEBS J* 281: 2353–2365, 2014. doi:10.1111/febs.12787.
21. **Crable SC, Hammond SM, Papes R, Rettig RK, Zhou GP, Gallagher PG, Joiner CH, Anderson KP.** Multiple isoforms of the KC1 cotransporter are expressed in sickle and normal erythroid cells. *Exp Hematol* 33: 624–631, 2005. doi:10.1016/j.exphem.2005.02.006.
22. **Daigle ND, Carpentier GA, Frenette-Cotton R, Simard MG, Lefoll MH, Noël M, Caron L, Noël J, Isenring P.** Molecular characterization of a human cation-Cl^- cotransporter (SLC12A8A, CCC9A) that promotes polyamine and amino acid transport. *J Cell Physiol* 220: 680–689, 2009. doi:10.1002/jcp.21814.
23. **Darman RB, Forbush B.** A regulatory locus of phosphorylation in the N terminus of the Na-K-Cl cotransporter, NKCC1. *J Biol Chem* 277: 37542–37550, 2002. doi:10.1074/jbc.M206293200.
24. **Davies SL, Roussa E, Le Rouzic P, Thévenod F, Alper SL, Best L, Brown PD.** Expression of K^+-Cl^- cotransporters in the alpha-cells of rat endocrine pancreas. *Biochim Biophys Acta* 1667: 7–14, 2004. doi:10.1016/j.bbamem.2004.08.005.
25. **Day RE, Kitchen P, Owen DS, Bland C, Marshall L, Conner AC, Bill RM, Conner MT.** Human aquaporins: regulators of transcellular water flow. *Biochim Biophys Acta* 1840: 1492–1506, 2014. doi:10.1016/j.bbagen.2013.09.033.
26. **De Braekeleer M, Dallaire A, Mathieu J.** Genetic epidemiology of sensorimotor polyneuropathy with or without agenesis of the corpus callosum in northeastern Quebec. *Hum Genet* 91: 223–227, 1993. doi:10.1007/BF00218260.
27. **De Franceschi L, Villa-Moruzzi E, Biondani A, Siciliano A, Brugnara C, Alper SL, Lowell CA, Berton G.** Regulation of K-Cl cotransport by protein phosphatase 1alpha in mouse erythrocytes. *Pflugers Arch* 451: 760–768, 2006. doi:10.1007/s00424-005-1502-7.
28. **de los Heros P, Alessi DR, Gourlay R, Campbell DG, Deak M, Macartney TJ, Kahle KT, Zhang J.** The WNK-regulated SPAK/OSR1 kinases directly phosphorylate and inhibit the K^+-Cl^- co-transporters. *Biochem J* 458: 559–573, 2014. doi:10.1042/BJ20131478.
29. **de Los Heros P, Kahle KT, Rinehart J, Bobadilla NA, Vázquez N, San Cristobal P, Mount DB, Lifton RP, Hebert SC, Gamba G.** WNK3 bypasses the tonicity requirement for K-Cl cotransporter activation via a phosphatase-dependent pathway. *Proc Natl Acad Sci USA* 103: 1976–1981, 2006. doi:10.1073/pnas.0510947103.
30. **Delpire E, Lauf PK.** Kinetics of Cl-dependent K fluxes in hyposmotically swollen low K sheep erythrocytes. *J Gen Physiol* 97: 173–193, 1991. doi:10.1085/jgp.97.2.173.
31. **Delpire E, Lu J, England R, Dull C, Thorne T.** Deafness and imbalance associated with inactivation of the secretory Na-K-2Cl co-transporter. *Nat Genet* 22: 192–195, 1999. doi:10.1038/9713.
32. **Di Fulvio M, Lauf PK, Adragna NC.** Nitric oxide signaling pathway regulates potassium chloride cotransporter-1 mRNA expression in vascular smooth muscle cells. *J Biol Chem* 276: 44534–44540, 2001. doi:10.1074/jbc.M104899200.
33. **Di Fulvio M, Lauf PK, Adragna NC.** The NO signaling pathway differentially regulates KCC3a and KCC3b mRNA expression. *Nitric Oxide* 9: 165–171, 2003. doi:10.1016/j.niox.2003.11.004.
34. **Di Fulvio M, Lincoln TM, Lauf PK, Adragna NC.** Protein kinase G regulates potassium chloride cotransporter-4 expression in primary cultures of rat vascular smooth muscle cells. *J Biol Chem* 276: 21046–21052, 2001. doi:10.1074/jbc.M100901200.
35. **Ding J, Delpire E.** Deletion of KCC3 in parvalbumin neurons leads to locomotor deficit in a conditional mouse model of peripheral neuropathy associated with agenesis of the corpus callosum. *Behav Brain Res* 274: 128–136, 2014. doi:10.1016/j.bbr.2014.08.005.
36. **Ding J, Ponce-Coria J, Delpire E.** A trafficking-deficient mutant of KCC3 reveals dominant-negative effects on K-Cl cotransport function. *PLoS One* 8: e61112, 2013. doi:10.1371/journal.pone.0061112.
37. **Dixon MJ, Gazzard J, Chaudhry SS, Sampson N, Schulte BA, Steel KP.** Mutation of the Na-K-Cl co-transporter gene *Slc12a2* results in deafness in mice. *Hum Mol Genet* 8: 1579–1584, 1999. doi:10.1093/hmg/8.8.1579.
38. **Dunham PB, Stewart GW, Ellory JC.** Chloride-activated passive potassium transport in human erythrocytes. *Proc Natl Acad Sci USA* 77: 1711–1715, 1980. doi:10.1073/pnas.77.3.1711.
39. **Dupre N, Howard HC, Rouleau GA.** Hereditary motor and sensory neuropathy with agenesis of the corpus callosum. In: *GeneReviews(R)*, edited by Pagon RA, Adam MP, Ardinger HH, Wallace SE, Amemiya A, Bean LJH, Bird TD, Ledbetter N, Mefford HC, Smith RJH, Stephens K. Seattle, WA: Univ. of Washington, 2006.
40. **Evans RL, Turner RJ.** Evidence for a physiological role of NH_4^+ transport on the secretory Na^+-K^+-$2Cl^-$ cotransporter. *Biochem Biophys Res Commun* 245: 301–306, 1998. doi:10.1006/bbrc.1998.8428.
41. **Flagella M, Clarke LL, Miller ML, Erway LC, Giannella RA, Andringa A, Gawenis LR, Kramer J, Duffy JJ, Doetschman T,**

Lorenz JN, Yamoah EN, Cardell EL, Shull GE. Mice lacking the basolateral Na-K-2Cl cotransporter have impaired epithelial chloride secretion and are profoundly deaf. *J Biol Chem* 274: 26946–26955, 1999. doi:10.1074/jbc.274.38.26946.

42. **Flemmer AW, Gimenez I, Dowd BF, Darman RB, Forbush B.** Activation of the Na-K-Cl cotransporter NKCC1 detected with a phospho-specific antibody. *J Biol Chem* 277: 37551–37558, 2002. doi:10.1074/jbc.M206294200.
43. **Foote JR, Behe P, Frampton M, Levine AP, Segal AW.** An exploration of charge compensating ion channels across the phagocytic vacuole of neutrophils. *Front Pharmacol* 8: 94, 2017. doi:10.3389/fphar.2017.00094.
44. **Frenette-Cotton R, Marcoux AA, Garneau AP, Noel M, Isenring P.** Phosphoregulation of K^+-Cl^- cotransporters during cell swelling: novel insights. *J Cell Physiol* 233: 396–408, 2018. doi:10.1002/jcp.25899.
45. **Fujii T, Takahashi Y, Itomi Y, Fujita K, Morii M, Tabuchi Y, Asano S, Tsukada K, Takeguchi N, Sakai H.** K^+-Cl^- cotransporter-3a upregulates Na^+,K^+-ATPase in lipid rafts of gastric luminal parietal cells. *J Biol Chem* 283: 6869–6877, 2008. doi:10.1074/jbc.M708429200.
46. **Gagnon KB.** High-grade glioma motility reduced by genetic knockdown of KCC3. *Cell Physiol Biochem* 30: 466–476, 2012. doi:10.1159/000339040.
47. **Gagnon KB, Di Fulvio M.** A molecular analysis of the Na^+-independent cation chloride cotransporters. *Cell Physiol Biochem* 32: 14–31, 2013. doi:10.1159/000356621.
48. **Gagnon KB, England R, Diehl L, Delpire E.** Apoptosis-associated tyrosine kinase scaffolding of protein phosphatase 1 and SPAK reveals a novel pathway for Na-K-2C1 cotransporter regulation. *Am J Physiol Cell Physiol* 292: C1809–C1815, 2007. doi:10.1152/ajpcell.00580.2006.
49. **Gamba G.** Molecular physiology and pathophysiology of electroneutral cation-chloride cotransporters. *Physiol Rev* 85: 423–493, 2005. doi:10.1152/physrev.00011.2004.
50. **Garneau AP, Marcoux AA, Noël M, Frenette-Cotton R, Drolet MC, Couet J, Larivière R, Isenring P.** Ablation of potassium-chloride cotransporter type 3 (Kcc3) in mouse causes multiple cardiovascular defects and isosmotic polyuria. *PLoS One* 11: e0154398, 2016. doi:10.1371/journal.pone.0154398.
51. **Garzón-Muvdi T, Pacheco-Alvarez D, Gagnon KB, Vázquez N, Ponce-Coria J, Moreno E, Delpire E, Gamba G.** WNK4 kinase is a negative regulator of K^+-Cl^- cotransporters. *Am J Physiol Renal Physiol* 292: F1197–F1207, 2007. doi:10.1152/ajprenal.00335.2006.
52. **Gerelsaikhan T, Turner RJ.** Transmembrane topology of the secretory Na^+-K^+-$2Cl^-$ cotransporter NKCC1 studied by in vitro translation. *J Biol Chem* 275: 40471–40477, 2000. doi:10.1074/jbc.M007751200.
53. **Gillen CM, Brill S, Payne JA, Forbush B III.** Molecular cloning and functional expression of the K-Cl cotransporter from rabbit, rat, and human. A new member of the cation-chloride cotransporter family. *J Biol Chem* 271: 16237–16244, 1996. doi:10.1074/jbc.271.27.16237.
54. **Glanville M, Kingscote S, Thwaites DT, Simmons NL.** Expression and role of sodium, potassium, chloride cotransport (NKCC1) in mouse inner medullary collecting duct (mIMCD-K2) epithelial cells. *Pflugers Arch* 443: 123–131, 2001. doi:10.1007/s004240100629.
55. **Gusev GP, Agalakova NI.** Regulation of K-Cl cotransport in erythrocytes of frog *Rana temporaria* by commonly used protein kinase and protein phosphatase inhibitors. *J Comp Physiol B* 180: 385–391, 2010. doi:10.1007/s00360-009-0418-5.
56. **Hall JE.** *Guyton and Hall Textbook of Medical Physiology* (13th ed.). New York: Saunders, 2016.
57. **Hiki K, D'Andrea RJ, Furze J, Crawford J, Woollatt E, Sutherland GR, Vadas MA, Gamble JR.** Cloning, characterization, and chromosomal location of a novel human K^+-Cl^- cotransporter. *J Biol Chem* 274: 10661–10667, 1999. doi:10.1074/jbc.274.15.10661.
58. **Hoffman JF.** Active transport of Na^+ and K^+ by red blood cells. In: *Membrane Physiology*, edited by Andreoli TE, Hoffman JF, Fanestil DD, and Schultz SG. New York: Springer, 1987, p. 221–234. doi:10.1007/978-1-4613-1943-6_13.
59. **Howard HC, Dubé MP, Prévost C, Bouchard JP, Mathieu J, Rouleau GA.** Fine mapping the candidate region for peripheral neuropathy with or without agenesis of the corpus callosum in the French Canadian population. *Eur J Hum Genet* 10: 406–412, 2002. doi:10.1038/sj.ejhg.5200815.
60. **Howard HC, Mount DB, Rochefort D, Byun N, Dupré N, Lu J, Fan X, Song L, Rivière JB, Prévost C, Horst J, Simonati A, Lemcke B, Welch R, England R, Zhan FQ, Mercado A, Siesser WB, George AL Jr, McDonald MP, Bouchard JP, Mathieu J, Delpire E, Rouleau GA.** The K-Cl cotransporter KCC3 is mutant in a severe peripheral neuropathy associated with agenesis of the corpus callosum. *Nat Genet* 32: 384–392, 2002. doi:10.1038/ng1002.
61. **Isenring P, Forbush B.** Ion transport and ligand binding by the Na-K-Cl cotransporter, structure-function studies. *Comp Biochem Physiol A Mol Integr Physiol* 130: 487–497, 2001. doi:10.1016/S1095-6433(01)00420-2.
62. **Isenring P, Jacoby SC, Forbush B III.** The role of transmembrane domain 2 in cation transport by the Na-K-Cl cotransporter. *Proc Natl Acad Sci USA* 95: 7179–7184, 1998. doi:10.1073/pnas.95.12.7179.
63. **Jennings ML, Adame MF.** Direct estimate of 1:1 stoichiometry of K^+-Cl^- cotransport in rabbit erythrocytes. *Am J Physiol Cell Physiol* 281: C825–C832, 2001.
64. **Kahle KT, Flores B, Bharucha-Goebel D, Zhang J, Donkervoort S, Hegde M, Begum G, Duran D, Liang B, Sun D, Bönnemann CG, Delpire E.** Peripheral motor neuropathy is associated with defective kinase regulation of the KCC3 cotransporter. *Sci Signal* 9: ra77, 2016. doi:10.1126/scisignal.aae0546.
65. **Klein T, Cooper TG, Yeung CH.** The role of potassium chloride cotransporters in murine and human sperm volume regulation. *Biol Reprod* 75: 853–858, 2006. doi:10.1095/biolreprod.106.054064.
66. **Kügler S, Meyn L, Holzmüller H, Gerhardt E, Isenmann S, Schulz JB, Bähr M.** Neuron-specific expression of therapeutic proteins: evaluation of different cellular promoters in recombinant adenoviral vectors. *Mol Cell Neurosci* 17: 78–96, 2001. doi:10.1006/mcne.2000.0929.
67. **Lang F, Vallon V, Knipper M, Wangemann P.** Functional significance of channels and transporters expressed in the inner ear and kidney. *Am J Physiol Cell Physiol* 293: C1187–C1208, 2007. doi:10.1152/ajpcell.00024.2007.
68. **Larbrisseau A, Vanasse M, Brochu P, Jasmin G.** The Andermann syndrome: agenesis of the corpus callosum associated with mental retardation and progressive sensorimotor neuronopathy. *Can J Neurol Sci* 11: 257–261, 1984. doi:10.1017/S0317167100045509.
69. **Lauf PK, Adragna NC.** Twenty-five years of K-Cl cotransport: from stimulation by a thiol reaction to cloning of the full-length KCCs. *Adv Exp Med Biol* 559: 11–28, 2004. doi:10.1007/0-387-23752-6_2.
70. **Lauf PK, Adragna NC, Dupre N, Bouchard JP, Rouleau GA.** K-Cl cotransport in red blood cells from patients with KCC3 isoform mutants. *Biochem Cell Biol* 84: 1034–1044, 2006. doi:10.1139/o06-203.
71. **Lauf PK, Theg BE.** A chloride dependent K^+ flux induced by N-ethylmaleimide in genetically low K^+ sheep and goat erythrocytes. *Biochem Biophys Res Commun* 92: 1422–1428, 1980. doi:10.1016/0006-291X(80)90445-3.
72. **Lauf PK, Warwar R, Brown TL, Adragna NC.** Regulation of potassium transport in human lens epithelial cells. *Exp Eye Res* 82: 55–64, 2006. doi:10.1016/j.exer.2005.05.002.
73. **Lauf PK, Zhang J, Delpire E, Fyffe RE, Mount DB, Adragna NC.** K-Cl co-transport: immunocytochemical and functional evidence for more than one KCC isoform in high K and low K sheep erythrocytes. *Comp Biochem Physiol A Mol Integr Physiol* 130: 499–509, 2001. doi:10.1016/S1095-6433(01)00421-4.
74. **Levick RJ.** *An Introduction to Cardiovascular Physiology* (5th ed.). Boca Raton, FL: CRC, 2010.
75. **Lin DH, Yue P, Rinehart J, Sun P, Wang Z, Lifton R, Wang WH.** Protein phosphatase 1 modulates the inhibitory effect of With-no-Lysine kinase 4 on ROMK channels. *Am J Physiol Renal Physiol* 303: F110–F119, 2012. doi:10.1152/ajprenal.00676.2011.
76. **Lucas O, Hilaire C, Delpire E, Scamps F.** KCC3-dependent chloride extrusion in adult sensory neurons. *Mol Cell Neurosci* 50: 211–220, 2012. doi:10.1016/j.mcn.2012.05.005.
77. **Lytle C, McManus TJ, Haas M.** A model of Na-K-2Cl cotransport based on ordered ion binding and glide symmetry. *Am J Physiol Cell Physiol* 274: C299–C309, 1998.
78. **Marangos PJ, Schmechel DE.** Neuron specific enolase, a clinically useful marker for neurons and neuroendocrine cells. *Annu Rev Neurosci* 10: 269–295, 1987. doi:10.1146/annurev.ne.10.030187.001413.
79. **Mathieu J, Bédard F, Prévost C, Langevin P.** [Motor and sensory neuropathies with or without agenesis of the corpus callosum: a radiological study of 64 cases]. *Can J Neurol Sci* 17: 103–108, 1990. doi:10.1017/S0317167100030298.
80. **Melo Z, Cruz-Rangel S, Bautista R, Vázquez N, Castañeda-Bueno M, Mount DB, Pasantes-Morales H, Mercado A, Gamba G.** Molecular evidence for a role for K^+-Cl^- cotransporters in the kidney. *Am J*

Physiol Renal Physiol 305: F1402–F1411, 2013. doi:10.1152/ajprenal.00390.2013.

81. **Melo Z, de los Heros P, Cruz-Rangel S, Vázquez N, Bobadilla NA, Pasantes-Morales H, Alessi DR, Mercado A, Gamba G.** N-terminal serine dephosphorylation is required for KCC3 cotransporter full activation by cell swelling. *J Biol Chem* 288: 31468–31476, 2013. doi:10.1074/jbc.M113.475574.
82. **Mercado A, de Los Heros P, Melo Z, Chávez-Canales M, Murillo-de-Ozores AR, Moreno E, Bazúa-Valenti S, Vázquez N, Hadchouel J, Gamba G.** With no lysine L-WNK1 isoforms are negative regulators of the K^+-Cl^- cotransporters. *Am J Physiol Cell Physiol* 311: C54–C66, 2016. doi:10.1152/ajpcell.00193.2015.
83. **Mercado A, Song L, Vazquez N, Mount DB, Gamba G.** Functional comparison of the K^+-Cl^- cotransporters KCC1 and KCC4. *J Biol Chem* 275: 30326–30334, 2000. doi:10.1074/jbc.M003112200.
84. **Mercado A, Vázquez N, Song L, Cortés R, Enck AH, Welch R, Delpire E, Gamba G, Mount DB.** NH_2-terminal heterogeneity in the KCC3 K^+-Cl^- cotransporter. *Am J Physiol Renal Physiol* 289: F1246–F1261, 2005. doi:10.1152/ajprenal.00464.2004.
85. **Meyer JW, Flagella M, Sutliff RL, Lorenz JN, Nieman ML, Weber CS, Paul RJ, Shull GE.** Decreased blood pressure and vascular smooth muscle tone in mice lacking basolateral Na^+-K^+-$2Cl^-$ cotransporter. *Am J Physiol Heart Circ Physiol* 283: H1846–H1855, 2002. doi:10.1152/ajpheart.00083.2002.
86. **Mollajew R, Zocher F, Horner A, Wiesner B, Klussmann E, Pohl P.** Routes of epithelial water flow: aquaporins versus cotransporters. *Biophys J* 99: 3647–3656, 2010. doi:10.1016/j.bpj.2010.10.021.
87. **Moore-Hoon ML, Turner RJ.** Molecular and topological characterization of the rat parotid Na^+-K^+-$2Cl^-$ cotransporter1. *Biochim Biophys Acta* 1373: 261–269, 1998. doi:10.1016/S0005-2736(98)00112-6.
88. **Mount DB, Mercado A, Song L, Xu J, George AL Jr, Delpire E, Gamba G.** Cloning and characterization of KCC3 and KCC4, new members of the cation-chloride cotransporter gene family. *J Biol Chem* 274: 16355–16362, 1999. doi:10.1074/jbc.274.23.16355.
89. **Orlov SN, Koltsova SV, Kapilevich LV, Dulin NO, Gusakova SV.** Cation-chloride cotransporters: regulation, physiological significance, and role in pathogenesis of arterial hypertension. *Biochemistry (Mosc)* 79: 1546–1561, 2014. doi:10.1134/S0006297914130070.
90. **Pan D, Kalfa TA, Wang D, Risinger M, Crable S, Ottlinger A, Chandra S, Mount DB, Hübner CA, Franco RS, Joiner CH.** K-Cl cotransporter gene expression during human and murine erythroid differentiation. *J Biol Chem* 286: 30492–30503, 2011. doi:10.1074/jbc.M110.206516.
91. **Payne JA.** Functional characterization of the neuronal-specific K-Cl cotransporter: implications for $[K^+]o$ regulation. *Am J Physiol Cell Physiol* 273: C1516–C1525, 1997.
92. **Payne JA, Stevenson TJ, Donaldson LF.** Molecular characterization of a putative K-Cl cotransporter in rat brain. A neuronal-specific isoform. *J Biol Chem* 271: 16245–16252, 1996. doi:10.1074/jbc.271.27.16245.
93. **Pearson MM, Lu J, Mount DB, Delpire E.** Localization of the K^+-Cl^- cotransporter, KCC3, in the central and peripheral nervous systems: expression in the choroid plexus, large neurons and white matter tracts. *Neuroscience* 103: 481–491, 2001. doi:10.1016/S0306-4522(00)00567-4.
94. **Piechotta K, Garbarini N, England R, Delpire E.** Characterization of the interaction of the stress kinase SPAK with the Na^+-K^+-$2Cl^-$ cotransporter in the nervous system: evidence for a scaffolding role of the kinase. *J Biol Chem* 278: 52848–52856, 2003. doi:10.1074/jbc.M309436200.
95. **Prosser CL.** *Comparative Animal Physiology* (4th ed.). Hoboken, NJ: John Wiley & Sons, 1991.
96. **Race JE, Makhlouf FN, Logue PJ, Wilson FH, Dunham PB, Holtzman EJ.** Molecular cloning and functional characterization of KCC3, a new K-Cl cotransporter. *Am J Physiol Cell Physiol* 277: C1210–C1219, 1999.
97. **Rambault A.** *FigTree v. 1.4.3* [Online]. Edinburgh, UK: Institute of Evolutionary Biology, University of Edinburgh. Software available at: http://tree.bio.ed.ac.uk/software/figtree. 2015.
98. **Rinehart J, Maksimova YD, Tanis JE, Stone KL, Hodson CA, Zhang J, Risinger M, Pan W, Wu D, Colangelo CM, Forbush B, Joiner CH, Gulcicek EE, Gallagher PG, Lifton RP.** Sites of regulated phosphorylation that control K-Cl cotransporter activity. *Cell* 138: 525–536, 2009. doi:10.1016/j.cell.2009.05.031.
99. **Rust MB, Alper SL, Rudhard Y, Shmukler BE, Vicente R, Brugnara C, Trudel M, Jentsch TJ, Hübner CA.** Disruption of erythroid K-Cl cotransporters alters erythrocyte volume and partially rescues erythrocyte dehydration in SAD mice. *J Clin Invest* 117: 1708–1717, 2007. doi:10.1172/JCI30630.
100. **Rust MB, Faulhaber J, Budack MK, Pfeffer C, Maritzen T, Didié M, Beck FX, Boettger T, Schubert R, Ehmke H, Jentsch TJ, Hübner CA.** Neurogenic mechanisms contribute to hypertension in mice with disruption of the K-Cl cotransporter KCC3. *Circ Res* 98: 549–556, 2006. doi:10.1161/01.RES.0000204449.83861.22.
101. **Salin-Cantegrel A, Rivière JB, Shekarabi M, Rasheed S, Dacal S, Laganière J, Gaudet R, Rochefort D, Lesca G, Gaspar C, Dion PA, Lapointe JY, Rouleau GA.** Transit defect of potassium-chloride cotransporter 3 is a major pathogenic mechanism in hereditary motor and sensory neuropathy with agenesis of the corpus callosum. *J Biol Chem* 286: 28456–28465, 2011. doi:10.1074/jbc.M111.226894.
102. **Salin-Cantegrel A, Shekarabi M, Rasheed S, Charron FM, Laganière J, Gaudet R, Dion PA, Lapointe JY, Rouleau GA.** Potassium-chloride cotransporter 3 interacts with Vav2 to synchronize the cell volume decrease response with cell protrusion dynamics. *PLoS One* 8: e65294, 2013. doi:10.1371/journal.pone.0065294.
103. **Sasaki S, Ishibashi K, Yoshiyama N, Shiigai T.** KCl co-transport across the basolateral membrane of rabbit renal proximal straight tubules. *J Clin Invest* 81: 194–199, 1988. doi:10.1172/JCI113294.
104. **Shekarabi M, Moldrich RX, Rasheed S, Salin-Cantegrel A, Laganière J, Rochefort D, Hince P, Huot K, Gaudet R, Kurniawan N, Sotocinal SG, Ritchie J, Dion PA, Mogil JS, Richards LJ, Rouleau GA.** Loss of neuronal potassium/chloride cotransporter 3 (KCC3) is responsible for the degenerative phenotype in a conditional mouse model of hereditary motor and sensory neuropathy associated with agenesis of the corpus callosum. *J Neurosci* 32: 3865–3876, 2012. doi:10.1523/JNEUROSCI.3679-11.2012.
105. **Shen MR, Chou CY, Ellory JC.** Volume-sensitive KCI cotransport associated with human cervical carcinogenesis. *Pflugers Arch* 440: 751–760, 2000. doi:10.1007/s004240000338.
106. **Shiozaki A, Takemoto K, Ichikawa D, Fujiwara H, Konishi H, Kosuga T, Komatsu S, Okamoto K, Kishimoto M, Marunaka Y, Otsuji E.** The K-Cl cotransporter KCC3 as an independent prognostic factor in human esophageal squamous cell carcinoma. *BioMed Res Int* 2014: 936401, 2014. doi:10.1155/2014/936401.
107. **Shmukler BE, Hsu A, Alves J, Trudel M, Rust MB, Hubner CA, Rivera A, Alper SL.** N-ethylmaleimide activates a Cl^--independent component of K^+ flux in mouse erythrocytes. *Blood Cells Mol Dis* 51: 9–16, 2013. doi:10.1016/j.bcmd.2013.02.004.
108. **Sievers F, Wilm A, Dineen D, Gibson TJ, Karplus K, Li W, Lopez R, McWilliam H, Remmert M, Söding J, Thompson JD, Higgins DG.** Fast, scalable generation of high-quality protein multiple sequence alignments using Clustal Omega. *Mol Syst Biol* 7: 539, 2011. doi:10.1038/msb.2011.75.
109. **Sigel E.** Use of *Xenopus* oocytes for the functional expression of plasma membrane proteins. *J Membr Biol* 117: 201–221, 1990. doi:10.1007/BF01868451.
110. **Simard CF, Bergeron MJ, Frenette-Cotton R, Carpentier GA, Pelchat ME, Caron L, Isenring P.** Homooligomeric and heterooligomeric associations between K^+-Cl^- cotransporter isoforms and between K^+-Cl^- and Na^+-K^+-Cl^- cotransporters. *J Biol Chem* 282: 18083–18093, 2007. doi:10.1074/jbc.M607811200.
111. **Simard CF, Brunet GM, Daigle ND, Montminy V, Caron L, Isenring P.** Self-interacting domains in the C terminus of a cation-Cl^- cotransporter described for the first time. *J Biol Chem* 279: 40769–40777, 2004. doi:10.1074/jbc.M406458200.
112. **Simon MM, Greenaway S, White JK, Fuchs H, Gailus-Durner V, Wells S, Sorg T, Wong K, Bedu E, Cartwright EJ, Dacquin R, Djebali S, Estabel J, Graw J, Ingham NJ, Jackson IJ, Lengeling A, Mandillo S, Marvel J, Meziane H, Preitner F, Puk O, Roux M, Adams DJ, Atkins S, Ayadi A, Becker L, Blake A, Brooker D, Cater H, Champy MF, Combe R, Danecek P, di Fenza A, Gates H, Gerdin AK, Golini E, Hancock JM, Hans W, Hölter SM, Hough T, Jurdic P, Keane TM, Morgan H, Müller W, Neff F, Nicholson G, Pasche B, Roberson LA, Rozman J, Sanderson M, Santos L, Selloum M, Shannon C, Southwell A, Tocchini-Valentini GP, Vancollie VE, Westerberg H, Wurst W, Zi M, Yalcin B, Ramirez-Solis R, Steel KP, Mallon AM, de Angelis MH, Herault Y, Brown SD.** A comparative

phenotypic and genomic analysis of C57BL/6J and C57BL/6N mouse strains. *Genome Biol* 14: R82, 2013. doi:10.1186/gb-2013-14-7-r82.

113. **Song L, Mercado A, Vázquez N, Xie Q, Desai R, George AL Jr, Gamba G, Mount DB.** Molecular, functional, and genomic characterization of human KCC2, the neuronal K-Cl cotransporter. *Brain Res Mol Brain Res* 103: 91–105, 2002. doi:10.1016/S0169-328X(02)00190-0.
114. **Strange K, Singer TD, Morrison R, Delpire E.** Dependence of KCC2 K-Cl cotransporter activity on a conserved carboxy terminus tyrosine residue. *Am J Physiol Cell Physiol* 279: C860–C867, 2000.
115. **Sun YT, Shieh CC, Delpire E, Shen MR.** K^+-Cl^- cotransport mediates the bactericidal activity of neutrophils by regulating NADPH oxidase activation. *J Physiol* 590: 3231–3243, 2012. doi:10.1113/jphysiol.2011.225300.
116. **Sun YT, Tzeng SF, Lin TS, Hsu KS, Delpire E, Shen MR.** KCC3 deficiency-induced disruption of paranodal loops and impairment of axonal excitability in the peripheral nervous system. *Neuroscience* 335: 91–102, 2016. doi:10.1016/j.neuroscience.2016.08.031.
117. **Thiel G, Greengard P, Südhof TC.** Characterization of tissue-specific transcription by the human synapsin I gene promoter. *Proc Natl Acad Sci USA* 88: 3431–3435, 1991. doi:10.1073/pnas.88.8.3431.
118. **Toye AA, Lippiat JD, Proks P, Shimomura K, Bentley L, Hugill A, Mijat V, Goldsworthy M, Moir L, Haynes A, Quarterman J, Freeman HC, Ashcroft FM, Cox RD.** A genetic and physiological study of impaired glucose homeostasis control in C57BL/6J mice. *Diabetologia* 48: 675–686, 2005. doi:10.1007/s00125-005-1680-z.
119. **Velázquez H, Silva T.** Cloning and localization of KCC4 in rabbit kidney: expression in distal convoluted tubule. *Am J Physiol Renal Physiol* 285: F49–F58, 2003. doi:10.1152/ajprenal.00389.2002.
120. **Wakamatsu S, Nonoguchi H, Ikebe M, Machida K, Izumi Y, Memetimin H, Nakayama Y, Nakanishi T, Kohda Y, Tomita K.** Vasopressin and hyperosmolality regulate NKCC1 expression in rat OMCD. *Hypertens Res* 32: 481–487, 2009. doi:10.1038/hr.2009.52.
121. **Wall SM, Trinh HN, Woodward KE.** Heterogeneity of NH_4^+ transport in mouse inner medullary collecting duct cells. *Am J Physiol Renal Physiol* 269: F536–F544, 1995.
122. **Wan G, Corfas G, Stone JS.** Inner ear supporting cells: rethinking the silent majority. *Semin Cell Dev Biol* 24: 448–459, 2013. doi:10.1016/j.semcdb.2013.03.009.
123. **Wang T, Delpire E, Giebisch G, Hebert S, Mount DB.** Impaired fluid and bicarbonate absorption in proximal tubules of KCC3 knockout mice (Abstract). *FASEB J* 17: A464, 2003.
124. **Warmuth S, Zimmermann I, Dutzler R.** X-ray structure of the C-terminal domain of a prokaryotic cation-chloride cotransporter. *Structure* 17: 538–546, 2009. doi:10.1016/j.str.2009.02.009.
125. **Watanabe M, Wake H, Moorhouse AJ, Nabekura J.** Clustering of neuronal K^+-Cl^- cotransporters in lipid rafts by tyrosine phosphorylation. *J Biol Chem* 284: 27980–27988, 2009. doi:10.1074/jbc.M109.043620.
126. **Weng TY, Chiu WT, Liu HS, Cheng HC, Shen MR, Mount DB, Chou CY.** Glycosylation regulates the function and membrane localization of KCC4. *Biochim Biophys Acta* 1833: 1133–1146, 2013. doi:10.1016/j.bbamcr.2013.01.018.
127. **Whitehead MC, Marangos PJ, Connolly SM, Morest DK.** Synapse formation is related to the onset of neuron-specific enolase immunoreactivity in the avian auditory and vestibular systems. *Dev Neurosci* 5: 298–307, 1982. doi:10.1159/000112689.
128. **Zhang J, Lauf PK, Adragna NC.** Platelet-derived growth factor regulates K-Cl cotransport in vascular smooth muscle cells. *Am J Physiol Cell Physiol* 284: C674–C680, 2003. doi:10.1152/ajpcell.00312.2002.